

## Discovery of a Potent, Selective, and Orally Active Phosphodiesterase 10A Inhibitor for the Potential Treatment of Schizophrenia

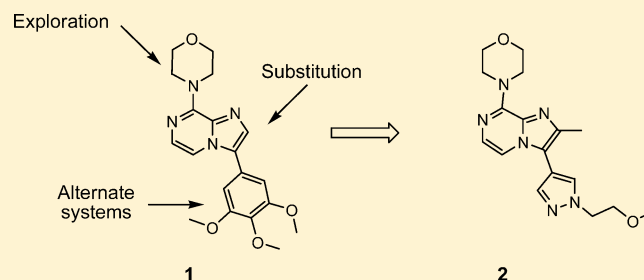
José Manuel Bartolomé-Nebreda,<sup>†</sup> Francisca Delgado,<sup>†</sup> María Luz Martín-Martín,<sup>†</sup> Carlos M. Martínez-Vituro,<sup>†</sup> Joaquín Pastor,<sup>†</sup> Han Min Tong,<sup>†</sup> Laura Iturrino,<sup>‡</sup> Gregor J. Macdonald,<sup>§</sup> Wendy Sanderson,<sup>||</sup> Anton Megens,<sup>⊥</sup> Xavier Langlois,<sup>⊥</sup> Marijke Somers,<sup>#</sup> Greet Vanhoof,<sup>∇</sup> and Susana Conde-Ceide<sup>\*,†</sup>

<sup>†</sup>Neuroscience Medicinal Chemistry and <sup>‡</sup>Discovery Sciences Analytical Sciences, Janssen Research & Development, Calle Jarama 75, Polígono Industrial, Toledo 45007, Spain

<sup>§</sup>Neuroscience Medicinal Chemistry, <sup>||</sup>Discovery Sciences Molecular Informatics, <sup>⊥</sup>Neuroscience Biology, <sup>#</sup>Discovery Sciences ADME/Tox, and <sup>∇</sup>Discovery Sciences Translational Sciences, Janssen Research & Development, Turnhoutseweg 30, B-2340, Beerse, Belgium

### S Supporting Information

**ABSTRACT:** We report the discovery of a series of imidazo[1,2-*a*]pyrazine derivatives as novel inhibitors of phosphodiesterase 10A (PDE10A). In a high-throughput screening campaign we identified the imidazopyrazine derivative **1**, a PDE10A inhibitor with limited selectivity versus the other phosphodiesterases (PDEs). Subsequent investigation of **1** and replacement of the trimethoxyphenyl group by a (methoxyethyl)pyrazole moiety maintained PDE10A inhibition but enhanced selectivity against the other PDEs. Systematic examination and analysis of structure–activity and structure–property relationships resulted in the discovery of **2**, an *in vitro* potent and selective inhibitor of PDE10A with high striatal occupancy of PDE10A, promising *in vivo* efficacy in different rodent behavioral models of schizophrenia, and a good pharmacokinetic profile in rats.



## ■ INTRODUCTION

Schizophrenia is a chronic and highly disabling mental illness characterized by a combination of positive (e.g., hallucinations and delusions), negative (e.g., anhedonia and poverty of speech), and cognitive (e.g., impaired attention and learning) symptoms,<sup>1</sup> which in the end limit the ability of patients to live an autonomous life. Despite tremendous progress in the management of schizophrenia since the introduction of current therapies, the so-called “typical” and “atypical” antipsychotics still suffer from several liabilities which limit their overall effectiveness in patients. All current medications act by blocking dopamine D<sub>2</sub> receptors, which drives their efficacy in treating the positive symptoms of the condition.<sup>2</sup> Unfortunately, they are not equally effective in all patient populations, and residual positive symptoms still remain for approximately 15% of patients.<sup>3</sup> Furthermore, current antipsychotics offer limited efficacy for the management of the negative symptoms and cognitive deficits of the disease. In addition, patient adherence and compliance to therapies is extremely poor<sup>4</sup> due to the wide range of side effects (e.g., Parkinson-like extrapyramidal symptoms (EPSs), prolactin release, weight gain, or even fatal cardiovascular events). As a consequence, there is a growing

interest in alternative mechanisms of action which do not involve direct interaction with dopaminergic receptors,<sup>5</sup> with the ultimate aim to develop therapeutics with both increased efficacy vs the core disease symptoms and improved tolerability.

Phosphodiesterases are a family of enzymes encoded by 21 genes and subdivided into 11 distinct families according to structural and functional properties. These enzymes metabolically inactivate widely occurring intracellular second messengers cyclic adenosine monophosphate (cAMP) and cyclic guanosine monophosphate (cGMP). These two second messengers regulate a wide variety of biological processes, including pro-inflammatory mediator production and action, ion channel function, muscle contraction, learning, differentiation, apoptosis, lipogenesis, glycogenolysis, and gluconeogenesis. The strength, duration, and location of cAMP and cGMP signaling are controlled by the different PDE enzymes.<sup>6</sup> Among the 11 family members, phosphodiesterase 10A (PDE10A) has been shown to hydrolyze both cAMP and cGMP with different kinetics<sup>7</sup> and to have the most restricted

Received: January 14, 2014

Published: April 23, 2014

distribution with high expression in the brain and testes.<sup>8</sup> In the brain, PDE10A mRNA and protein are highly expressed in striatal medium spiny neurons (MSNs). Medium spiny neurons are key for transmission and control of glutamatergic and dopaminergic input within the basal ganglia and form key output pathways that help discriminate relevant and irrelevant cognitive and motor patterns.<sup>9</sup> Thus, MSNs are  $\gamma$ -aminobutyric acidergic (GABAergic) projection neurons evenly distributed between two distinct pathways—striatonigral MSNs (in the direct pathway), which express the D<sub>1</sub> dopamine receptor, and striatopallidal MSNs (in the indirect pathway), which express the D<sub>2</sub> dopamine receptors. Ultimately, as D<sub>1</sub> dopamine receptors are positively coupled to cAMP production and D<sub>2</sub> dopamine receptors are negatively coupled to cAMP production, a putative increase in cAMP concentration in these pathways via inhibition of PDE10A would mimic the effect of D<sub>1</sub> agonism and D<sub>2</sub> antagonism. The unique role of PDE10A in the brain, together with its increased pharmacological characterization, has prompted enormous interest in investigating the potential of inhibitors for treating neurological and psychiatric disorders such as schizophrenia.<sup>10</sup>

After the pioneering work by Pfizer to characterize the PDE10A inhibitory properties of papaverine,<sup>11</sup> numerous companies have reported PDE10A inhibitors from different structural classes.<sup>12</sup> Furthermore, following the reported pharmacological profile of Pfizer's TP-10<sup>13</sup> (Figure 1), efficacy

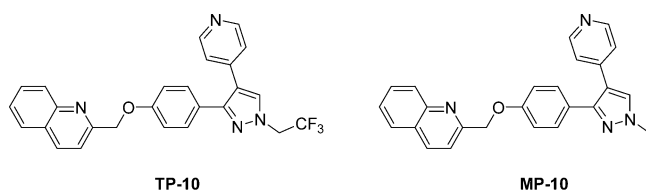


Figure 1. Structures of TP-10 and MP-10.

in various in vivo models predictive for antipsychotic activity has been reported for many different PDE10A inhibitors.<sup>14</sup> Moreover, PF-02545920 or MP-10 (Figure 1), which is a structurally related analogue of TP-10 with a promising human pharmacokinetic profile,<sup>15</sup> is currently being evaluated by Pfizer in phase IIa studies. Although MP-10 failed to show efficacy as a monotherapy in the acute exacerbation of schizophrenia,<sup>16</sup> it is currently being investigated as an adjunctive therapy in patients with schizophrenia who failed to respond adequately to treatment with antipsychotics alone.<sup>17</sup> Furthermore, several other PDE10A inhibitors are currently undergoing clinical investigation,<sup>18</sup> and hence, it remains to be proven whether PDE10A inhibitors may represent a viable therapy for the symptoms of schizophrenia or other neurological disorders such as Huntington's disease (HD)<sup>19</sup> or Lesch–Nyhan disease.<sup>20</sup>

Among a series of imidazo[1,2-*a*]pyrazine-containing compounds that were identified through a high-throughput screen as having inhibitory activity against the PDE10A enzyme, our initial hit **1** showed good potency (PDE10A pIC<sub>50</sub> = 6.8) but limited selectivity versus the other PDEs (see Figure 4). Despite this suboptimal selectivity, compound **1** (Figure 2) was selected as a viable starting point for a CNS-focused exploration given its promising PDE10A inhibition and attractive physicochemical properties (MW = 328; TPSA = 69). Starting from compound **1**, we undertook the lead optimization program outlined in Figure 2, aimed to improve the overall

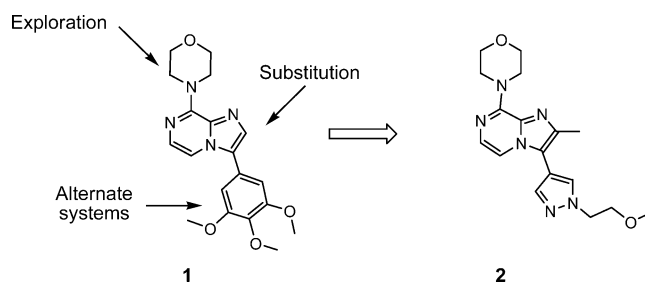


Figure 2. Structures of **1** and **2**.

in vitro and in vivo profile. The in vitro pharmacology and absorption, distribution, metabolism, and excretion (ADME) parameters determined for compounds synthesized in this lead optimization campaign are provided in Tables 1–3, with in vivo pharmacology and pharmacokinetic data detailed in Tables 4 and 5. This work culminated in the discovery and characterization of **2** (Figure 2) as a potent, selective brain penetrant and orally active PDE10A inhibitor.

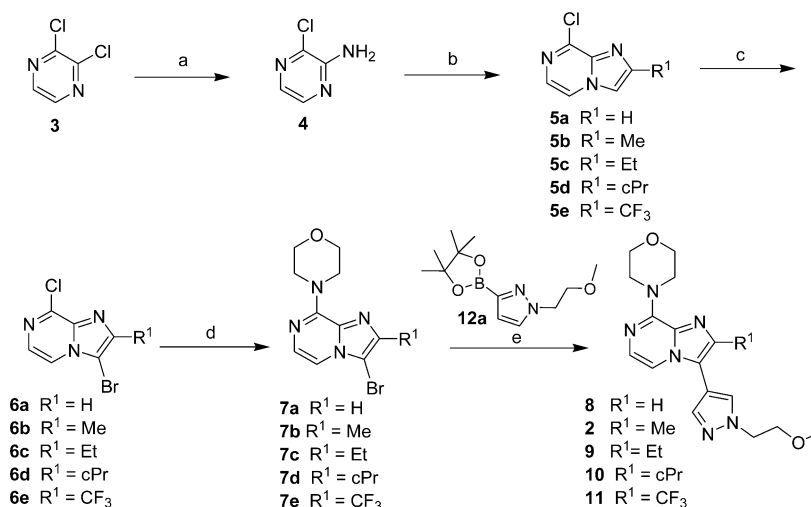
## CHEMISTRY

The syntheses of the imidazo[1,2-*a*]pyrazine derivatives are outlined in Schemes 1–6.

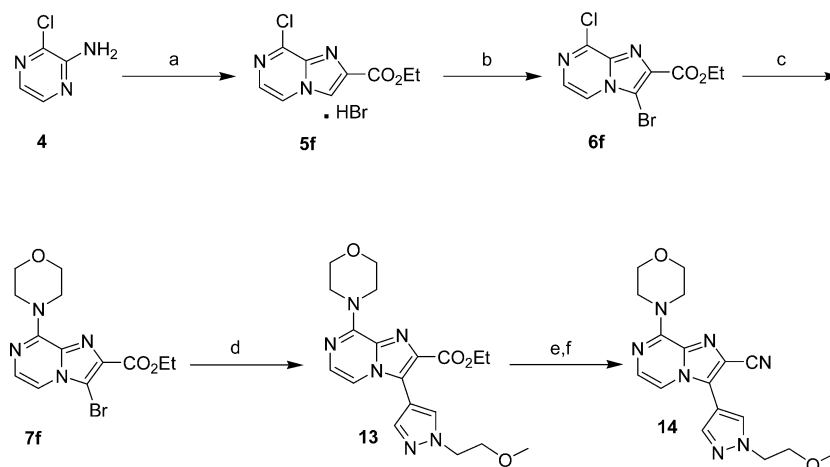
Compounds **2** and **8–11** were prepared following the synthetic route depicted in Scheme 1. Thus, treatment of commercially available 1,2-dichloropyrazine (**3**) with an aqueous solution of ammonium hydroxide afforded **4**, which was then condensed with the corresponding  $\alpha$ -halocarbonyl derivatives to build the imidazo[1,2-*a*]pyrazine cores **5**. In the case of **5e**, the cyclization reaction took place with hydrolysis of the chlorine atom and required treatment of the intermediate formed with POCl<sub>3</sub> to afford the desired intermediate. Selective bromination at the 3-position was achieved in good yields with NBS, as previously described in the literature,<sup>21</sup> to afford intermediates **6**, which were then reacted with morpholine to give key precursors **7**. In parallel, the alkylation of 4-(4,4,5,5-tetramethyl[1,3,2]dioxaborolan-2-yl)-1*H*-pyrazole (**12**) with 2-chloroethyl methyl ether using cesium carbonate as the base afforded the required 1-(2-methoxyethyl)-4-(4,4,5,5-tetramethyl[1,3,2]dioxaborolan-2-yl)-1*H*-pyrazole (**12a**). Finally, Suzuki–Miyaura palladium-catalyzed cross-coupling of intermediates **7** with 1-(2-methoxyethyl)-4-(4,4,5,5-tetramethyl[1,3,2]dioxaborolan-2-yl)-1*H*-pyrazole (prepared by reaction of commercially available 4,4,5,5-tetramethyl[1,3,2]dioxaborolan-2-yl)-1*H*-pyrazole with 2-chloroethyl methyl ether in the presence of cesium carbonate as the base in DMF at 160 °C under microwave irradiation) afforded the targeted compounds **2** and **8–11** (Scheme 1).

In the case of compound **14**, the reaction of **4** with ethyl bromopyruvate afforded, as in the previous cases, the corresponding imidazo[1,2-*a*]pyrazine core **5f**. Selective bromination of **5f** followed by introduction of the morpholine afforded **7f**, which was then reacted with **12a** via Suzuki–Miyaura coupling to provide intermediate **13**. Finally, reaction of **13** with ammonium hydroxide followed by dehydration of the intermediate primary amide with phosphorus oxychloride afforded the desired nitrile derivative **14**.

In the case of compound **17**, we followed a slightly modified route. Compound **4** was reacted with morpholine to afford precursor **15**, which was then condensed with bromoacetic acid to yield the corresponding 2-hydroxy intermediate. This was subsequently alkylated with methyl iodide, under basic

Scheme 1. Synthesis of Compounds 2 and 8–11<sup>a</sup>

<sup>a</sup>Reagents and conditions: (a) NH<sub>4</sub>OH, 100 °C, 24 h, 90%; (b) for compound **5a** bromoacetaldehyde diethyl acetal, HBr, NaHCO<sub>3</sub>, iPrOH, 70%; for compound **5b** chloroacetone, 90 °C, 18 h, 68.5%; for compound **5c** 1-bromo-2-butanone, 90 °C, 18 h, 100%; for compound **5d** 2-bromo-1-cyclopropylethanone, ACN, 90 °C, 24 h, 38%; for compound **5e** (i) 1-chloro-3,3,3-trifluoroacetone, 100 °C, 16 h, 39%; (ii) POCl<sub>3</sub>, *N,N*-dimethylaniline, 90 °C, 4 h, 99%; (c) NBS, DCM, rt, 2 h; 73–100%; (d) morpholine, DIPEA, ACN, 80 °C, 7 h, 48–99%; (e) 1-(2-methoxyethyl)-4-(4,4,5,5-tetramethyl[1,3,2]dioxaborolan-2-yl)-1*H*-pyrazole, Pd(OAc)<sub>2</sub>, PPh<sub>3</sub>, K<sub>2</sub>CO<sub>3</sub>, 1,4-dioxane, 80 °C, 16 h, 28–85%.

Scheme 2. Synthesis of Compound 14<sup>a</sup>

<sup>a</sup>Reagents and conditions: (a) ethyl bromopyruvate, DME, rt, 2.5 h, 92%; (b) NBS, DCM, rt, 2 h, 83%; (c) morpholine, DIPEA, ACN, 80 °C, 7 h, 99%; (d) **12a**, Pd(PPh<sub>3</sub>)<sub>4</sub>, Na<sub>2</sub>CO<sub>3</sub>, 1,4-dioxane, 80 °C, 16 h, 28%; (e) NH<sub>4</sub>OH, 80 °C, 16 h, 28%; (f) POCl<sub>3</sub>, 80 °C, 1 h, 39%.

conditions, to afford compound **16**. Selective bromination of **16** at the 3-position was achieved in good yields using NBS to yield **7g**, which after Suzuki–Miyaura-type cross-coupling with the corresponding boronate **12a** afforded the target compound **17** (Scheme 3).

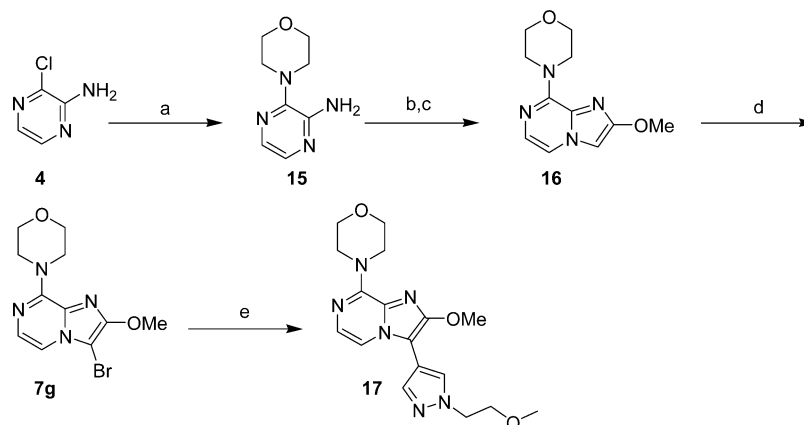
The general route for the synthesis of compounds **18–26** is outlined in Scheme 4. Suzuki–Miyaura coupling of bromide **7b** with the corresponding pyrazole-containing boronates, analogously to the preparation of compound **8**, yielded the desired analogues **18–26** (Scheme 4) in moderate to high yields. Boronate **12d** was commercially available, while the other boronate derivatives **12b,c,e–j** were prepared by an alkylation reaction of 4-(4,4,5,5-tetramethyl[1,3,2]dioxaborolan-2-yl)-1*H*-pyrazole with the corresponding halo or tosyl derivatives which were either commercially available or prepared following the procedures described above.

For the synthesis of compounds **29** and **30**, the reaction of **7b** with the commercially available **27** accompanied by in situ deprotection of the Boc protecting group afforded in one step compound **28**. The reaction of **28** with 1-chloro-2,2-dimethyl-2-propanol followed by alkylation with dimethyl sulfate, in the presence of sodium hydride, yielded the desired analogue **29**. Finally, the reaction of **28** with ethyl iodide, using cesium carbonate as the base, afforded compound **30**.

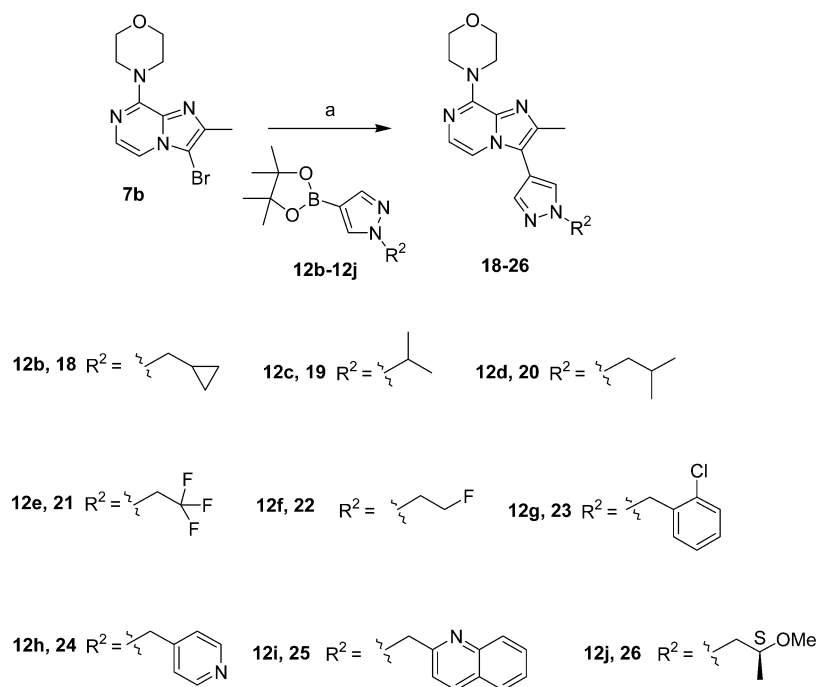
Compound **32** was prepared similarly to compound **8**, with morpholine being replaced by pyrrolidine. For compounds **35** and **36**, the pyridyl moiety was introduced by Suzuki–Miyaura cross-coupling with the corresponding pyridylboronic acid derivatives (Scheme 6) on the intermediate **5b**.

## RESULTS AND DISCUSSION

After a structural analysis of multiple families of different PDE inhibitors, we postulated that the limited selectivity observed

Scheme 3. Synthesis of Compound 17<sup>a</sup>

<sup>a</sup>Reagents and conditions: (a) morpholine, 120 °C, 16 h, 84%; (b) bromoacetic acid, 2-propanol, 90 °C, 16 h, 77%; (c) MeI, Cs<sub>2</sub>CO<sub>3</sub>, DMF, rt, 1 h, 39%; (d) NBS, DCM, 0 °C, 2 h, 86%; (e) **12a**, Pd(PPh<sub>3</sub>)<sub>4</sub>, Na<sub>2</sub>CO<sub>3</sub>, 1,4-dioxane, 80 °C, 16 h, 38%.

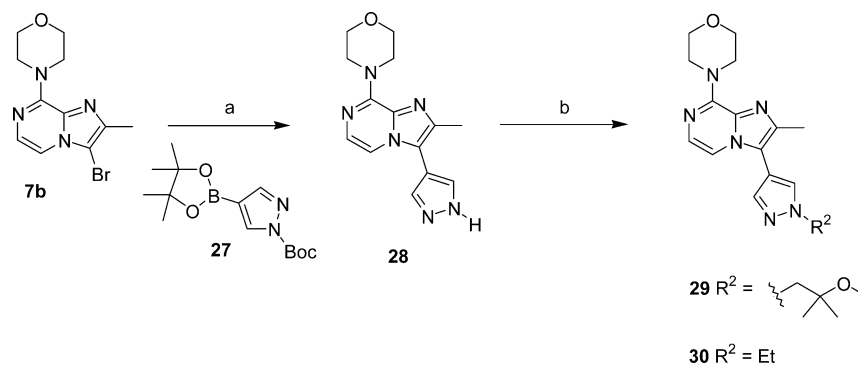
Scheme 4. Synthesis of Compounds 18–26<sup>a</sup>

<sup>a</sup>Reagents and conditions: (a) Pd(OAc)<sub>2</sub>, PPh<sub>3</sub>, K<sub>2</sub>CO<sub>3</sub>, 1,4-dioxane, 80 °C, 16 h or [1,1'-bis(diphenylphosphino)ferrocene]dichloropalladium(II), Cs<sub>2</sub>CO<sub>3</sub>, DME/H<sub>2</sub>O, 140 °C, microwave irradiation, 30 min, 34–98%.

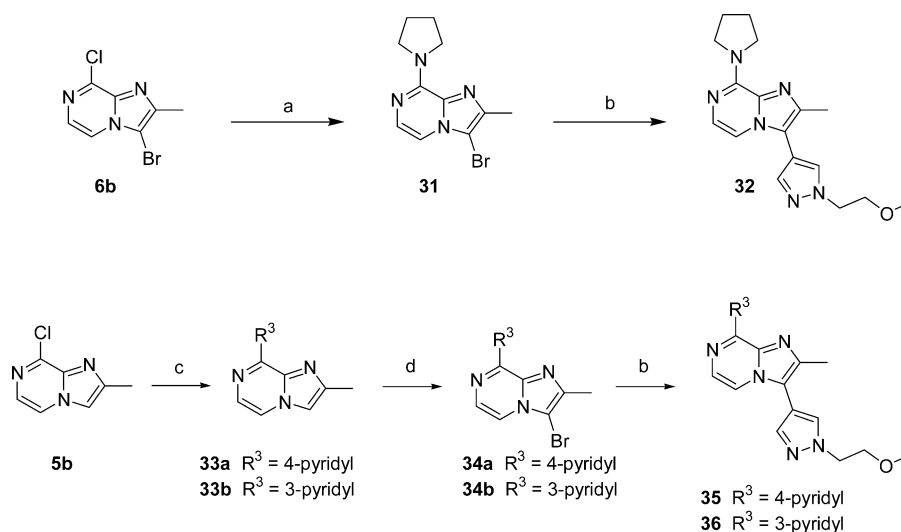
with compound **1** (Figure 4) could be due to the presence of the trimethoxyphenyl group, as dialkoxyaryl motives are common to several other PDE inhibitors.<sup>22</sup> In previously reported catechol-containing PDE inhibitors, the two alkoxy groups form a bidentate hydrogen bond interaction with the NH of glutamine Gln716, which is a well-preserved residue across all members of the PDE families.

The possible binding mode of molecule **1** was examined by a manual docking placement procedure into the PDE10A protein. The apo-PDE10A structure (PDB 2O8H) was prepared in MOE.<sup>23</sup> Initially, all of the solvent was retained, and the extent of water displacement was considered in a manual and iterative way, removing waters as necessary. The ligand was placed in alternative orientations with emphasis on maintaining adequate volume occupancy of the active site,

reproducing the key interaction with Gln716, and considering protein–ligand interactions, especially those formed in place of protein–solvent interactions. Two possible binding modes were identified for compound **1** (see Figure 3). The first, mode A, is a more classical PDE–methoxyphenyl protein–ligand interaction wherein the two methoxy groups form a bidentate interaction with the NH of Gln716 and the morpholine group projects toward the solvent, forming hydrophobic interactions with Ser561 and Met703. The second, mode B, is an alternative binding mode where the morpholine group extends into a small PDE10A-specific pocket called Q1, while the N of the imidazole makes an interaction with the NH of Gln716. This latter mode is less expected; however, an in-house PDE10 X-ray structure of a structurally related trimethoxyphenyl derivative (unpublished results) shows this binding orientation, and the

Scheme 5. Synthesis of Compounds 29 and 30<sup>a</sup>

<sup>a</sup>Reagents and conditions: (a) Pd(OAc)<sub>2</sub>, PPh<sub>3</sub>, K<sub>2</sub>CO<sub>3</sub>, 1,4-dioxane, 80 °C, 16 h, 81%; (b) for **29** (i) 1-chloro-2-methyl-2-propanol, Cs<sub>2</sub>CO<sub>3</sub>, DMF, 160 °C, microwave irradiation, 40 min, 82%; (ii) dimethyl sulfate, NaH, THF, 70 °C, 18 h, 39%; for **30** ethyl iodide, Cs<sub>2</sub>CO<sub>3</sub>, DMF, 160 °C, microwave irradiation, 40 min, 62%.

Scheme 6. Synthesis of Compounds 32, 35, and 36<sup>a</sup>

<sup>a</sup>Reagents and conditions: (a) pyrrolidine, DIPEA, ACN, 80 °C, 7 h, 85%; (b) **12a**, Pd(OAc)<sub>2</sub>, PPh<sub>3</sub>, Na<sub>2</sub>CO<sub>3</sub>, 1,4-dioxane, 80 °C, 16 h, 23–58%; (c) 3-pyridylboronic acid or 4-pyridylboronic acid, Pd(OAc)<sub>2</sub>, PPh<sub>3</sub>, Na<sub>2</sub>CO<sub>3</sub>, 1,4-dioxane, 80 °C, 16 h, 53–63%; (d) NBS, DCM, rt, 2 h, 86–89%.

modeling suggests it is also plausible for this chemical series. In this case, the trimethoxyphenyl ring is oriented toward the solvent and interacts mostly with Met703, but also with the edge of Phe719. This is one of the two phenylalanine residues, together with Phe686, which form a well-reported hydrophobic clamp in different PDE inhibitors which holds the imidazo[1,2-*a*]pyrazine core in place via a favorable face-to-face interaction with Phe719 on one side and an edge-to-face interaction with Phe686 on the other side. On the basis of this analysis, we considered replacing the potentially promiscuous trimethoxyphenyl group by other moieties that could retain significant PDE10A inhibitory activity with enhanced selectivity. We hoped to achieve this by eliminating the dialkoxy interaction with glutamine Gln716 and forcing a mode B-type binding mode (Figure 3).

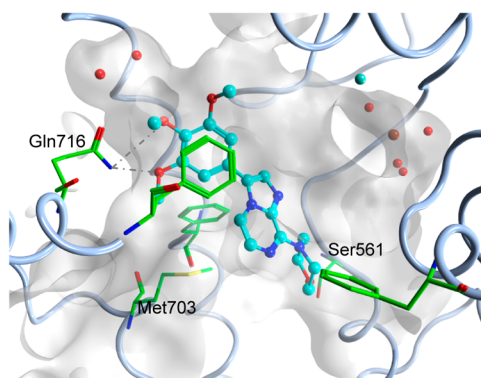
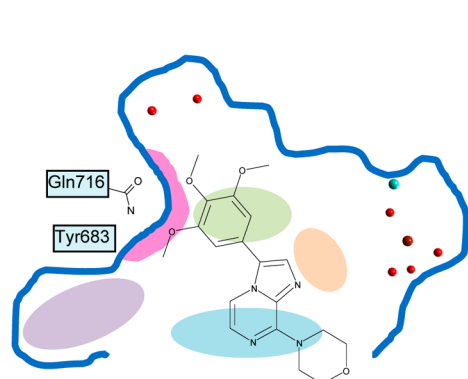
Detailed structural and overlapping analyses of different hits which emerged from the HTS campaign and in which the trimethoxyaryl group was not present revealed a potentially good overlap between the trimethoxyphenyl of **1** and a (methoxyethyl)pyrazole group present in another structurally related series (unpublished results). Hits from these series displayed a hydrogen bond between Gln716 and a nitrogen

atom present in the heterocyclic core similar to the N1 of the imidazo[1,2-*a*]pyrazine, providing more support for binding mode B (Figure 3).

In light of these similarities, we hypothesized that the (methoxyethyl)pyrazole moiety could represent a good replacement for the trimethoxyphenyl group, and with this rationale in mind, we targeted hybrid compound **8**. Confirming our design principle, compound **8**, despite showing a decrease in PDE10A inhibition (PDE10A pIC<sub>50</sub> = 6.0) compared to **1**, indeed possessed reduced potency at the other members of the PDE family (other PDEs pIC<sub>50</sub> < 5) (Figure 4).

Encouraged by this result and with the aim to improve PDE10A inhibition, we decided to explore the effect of substitution in different positions around the bicyclic imidazo[1,2-*a*]pyrazine scaffold in **8**. Our initial SAR efforts were directed toward the introduction of diverse moieties at the 2-position. Small substituents in this position were generally found to be well-tolerated, resulting in an increase in PDE10A inhibition potency. In particular, the introduction of small alkyl substituents such as methyl, ethyl, or cyclopropyl, providing compounds **2**, **9**, and **10**, respectively, resulted in an increased in vitro inhibition (0.8–1.2 log units). A significant increase in

## Mode A



## Mode B

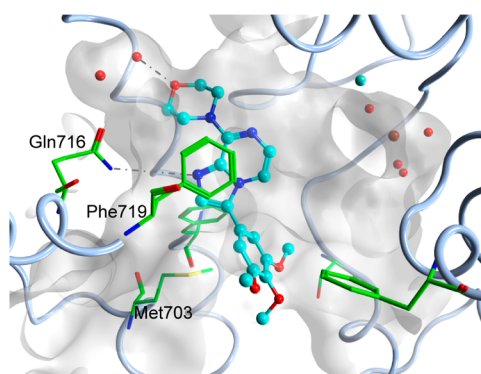
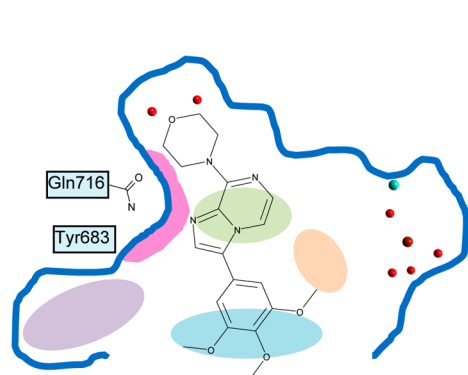
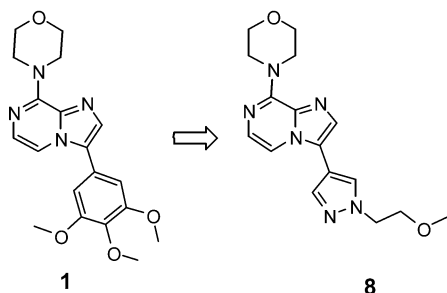


**Figure 3.** 2D and 3D representations of two possible binding modes of **1** in the apo-PDE10 structure (PDB code 2O8H). The 2D representation shows regions of importance for PDE10A inhibition: Gln interaction (magenta), selectivity pocket (purple), hydrophobic clamp (green), ribose region (orange), exo-binding region (cyan), buried waters (small red dots), and metal site (big red and cyan dots).<sup>24</sup>



| PDE type                       | 10A | 1B  | 3A  | 5A  | 6A  | Others |
|--------------------------------|-----|-----|-----|-----|-----|--------|
| pIC <sub>50</sub> ( <b>1</b> ) | 6.8 | 5.6 | 5.8 | 6.0 | 6.0 | <5     |
| pIC <sub>50</sub> ( <b>8</b> ) | 6.0 | <5  | <5  | <5  | <5  | <5     |

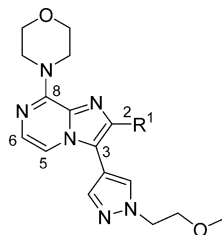
**Figure 4.** Structure and PDE selectivity of compounds **1** and **8**.

activity was also achieved with compound **14**, which bears the strong electron-withdrawing cyano group, while the effect was less pronounced for compound **11**, which bears the more lipophilic electron-withdrawing trifluoromethyl moiety. By contrast, the introduction of a strongly electron-donating methoxy substituent, as in compound **17**, had only marginal effects on the in vitro potency with respect to prototype **8**. In light of their attractive in vitro potencies, compounds **2**, **9–11**, and **14** were further investigated for their ability to inhibit PDE10A in vivo. As the effect of PDE10A inhibition in vivo is expected to be similar to that of D<sub>2</sub> receptor blockade, we decided to investigate these compounds against apomorphine-induced stereotypy in rats, a well-validated model that has been extensively used to evaluate D<sub>2</sub> receptor blockers.<sup>25</sup> Thus, following subcutaneous (sc) administration, all tested com-

pounds (except **11**) were able to revert the effects of apomorphine at doses of <10 mg/kg (chosen as a cutoff criterion). Additionally, as shown in Table 1, the metabolic stability of this set of compounds was evaluated in rat liver microsomes (RLMs) after 15 min of incubation at 1 μM concentration. Among this set, compound **2** provided the most balanced profile with improved in vitro and in vivo potencies together with good microsomal stability and was therefore considered an attractive lead for further investigation.

As a continuation of our SAR strategy, investigations were then focused on an exploration of the pyrazole side chain, taking compound **2** as the starting point. A wide variety of differently substituted side chains were investigated,<sup>26</sup> and selected results from this exploration are summarized in Table 2. The deletion of the methoxy group (compound **30**) slightly

Table 1. PDE10A Inhibitory Activity of the Modifications at C2



| compd | R <sup>1</sup>  | PDE10A pIC <sub>50</sub> ± SD <sup>a</sup> | apo ED <sub>50</sub> <sup>b</sup> (mg/kg) | RLM <sup>c</sup> (%) |
|-------|-----------------|--|---|----------------------|
| 2     | Me              | 6.85 ± 0.14                                | 3.6 (2.8–4.4) <sup>d</sup>                | 23                   |
| 9     | Et              | 6.81 ± 0.17                                | 5.0 (2.9–8.7)                             | 54                   |
| 10    | cyclopropyl     | 7.27 ± 0.16                                | 5.0 (2.9–8.7)                             | 64                   |
| 14    | CN              | 7.07 ± 0.11                                | 5.0 (2.9–8.7)                             | 57                   |
| 11    | CF <sub>3</sub> | 6.51 ± 0.06                                | >10                                       | 40                   |
| 17    | MeO             | 6.59 ± 0.20 (n = 1) <sup>d</sup>           | nt <sup>e</sup>                           | 42                   |

<sup>a</sup>Values are the mean ± SD of at least three experiments. <sup>b</sup>Wiga rats (n = 3) were pretreated with test compound (sc) or solvent, and after 30 min, apomorphine (1.0 mg/kg, iv) induced stereotypy was scored every 5 min over the first hour after injection of apomorphine. <sup>c</sup>RLM data refer to the percentage of compound metabolized after incubation of the tested compound with rat liver microsomes for 15 min at 1 μM concentration. <sup>d</sup>n = 5. <sup>e</sup>Not tested.

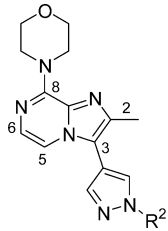
decreased the in vitro and in vivo activity, while other bulkier alkyl side chains, such as cyclopropylmethyl, isopropyl, and isobutyl (compounds 18, 19, and 20, respectively), were better tolerated. This would indicate that the size of the side chain may be important for in vitro activity, probably due to increased lipophilic interactions. In vivo evaluation of this set revealed that compound 20 was the most potent, as it was able to revert the effects of apomorphine at a dose of 2 mg/kg sc. However, metabolic stability of this compound in RLMs was low (87% metabolized after 15 min of incubation at 1 μM concentration). Interestingly, increases in the in vitro PDE10A potencies were also obtained through the introduction of fluoroalkyl groups, as in compounds 21 and 22. While the trifluoroethyl analogue 21 showed good metabolic stability (30% metabolized), the corresponding fluoroethyl congener 22 showed poor metabolic stability (68% metabolized), which precluded further investigation. On the basis of previous results and aiming to access an additional face–edge interaction with the previously mentioned Phe686 (vide supra),<sup>27</sup> we incorporated aryl- and heteroaryl-containing side chains (compounds 23–25). The 2-chlorobenzyl group in compound 23 was included as the interaction between this group and Phe686 was confirmed for another unrelated series that we were exploring in parallel (unpublished results). Although compound 23 showed comparable in vitro potency, it lacked adequate metabolic stability and in vivo activity in the apomorphine model. Similar results were obtained for compounds 24 and 25, where the introduction of pyridine and quinoline rings resulted in a significant decrease in in vivo activity (ED<sub>50</sub> > 10 mg/kg sc). Ultimately, the best results were obtained by the introduction of a methyl substituent or a gem-dimethyl substituent in the α position to the methoxy group in compounds 26 (due to the accessibility of the starting materials, the S-enantiomer was selected as a representative example) and 29. These compounds, despite maintaining in vitro potencies comparable to other members of this set and offering a significant improvement in in vivo activity, unfortunately lacked sufficient metabolic stability (>65% metabolized) and were discarded for further profiling.

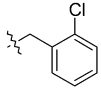
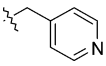
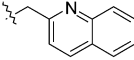
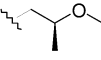
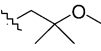
To better understand the most relevant binding features of our imidazo[1,2-a]pyrazine series, the cocrystal structure of

PDE10A (human) complexed with compound 26 as a representative example (Figure 5) was obtained. This crystal structure revealed a typical PDE binding mode for both monomers in the asymmetric unit with the imidazo[1,2-a]pyrazine scaffold held in place by the already mentioned phenylalanine clamp. In addition, hydrogen-bonding interactions were formed between the N1 of the imidazo[1,2-a]pyrazine and the NH of the preserved Gln716. The morpholine group extended into the Q1 pocket, while the R group on the pyrazole extended toward the solvent, allowing the methoxy group to interact with Phe629 in the lid region of the active site. This relatively nonspecific hydrophobic interaction with Phe629, in combination with differences in entropy loss upon binding, may explain the relatively unresponsive in vitro pyrazole side chain SAR. Finally, although the active site contains two metal atoms, Zn(II) and Mg(II), 26 does not interact with either of them.

Subsequent SAR exploration of compound 2 was centered on studying the effects of the replacement of the morpholine group at position 8 of the imidazo[1,2-a]pyrazine core by other diverse groups (small alkyls, amines, ethers, and heterocycles). Out of this exploration, only three compounds showed PDE10A pIC<sub>50</sub> > 6.0 (see Table 3). According to the X-ray structure of the complex of 26 with the PDE10A enzyme, the oxygen of the morpholine would form a hydrogen bond with one of the conserved water molecules in the Q1 pocket (Figure 5). This conserved water molecule is bonded to Thr675 and another conserved water molecule, which in turn is bonded to Trp752 and the conserved Gln716. Interestingly, replacement of the morpholine by a pyrrolidine, which is unsuitable for this H-bonding interaction (compound 32), resulted in a decrease of in vitro potency. An overlay of the X-ray structures of compound 26 and MP-10<sup>28</sup> (Figure 6) showed that the pyridine nitrogen of MP-10 could also act as a hydrogen bond acceptor to the conserved water molecule in the Q1 pocket that is hydrogen bonded to the PDE10A backbone. In analogy, we targeted the 4- and 3-pyridine derivatives 35 and 36, respectively. From the data in Table 3, compound 35 was found to be more active than 36, which could be explained by the crystal structure where the pyridyl nitrogen in compound 35 may be better oriented to form the hydrogen bond to the

Table 2. PDE10A Inhibitory Activity of the Modifications of the Side Chain of the Pyrazole



| Compound | R <sup>2</sup>  | PDE10A                             | APO                                   | RLM               |
|----------|---|------------------------------------|---------------------------------------|-------------------|
|          |   | pIC <sub>50</sub> ±SD <sup>a</sup> | ED <sub>50</sub> (mg/kg) <sup>b</sup> | (%) <sup>c</sup>  |
| 30       | Et  | 6.63±0.15                          | 7.9 (3.6-17)                          | n.t. <sup>d</sup> |
| 18       |    | 7.19±0.09                          | >10                                   | 57                |
| 19       | isopropyl   | 6.95±0.14                          | >10                                   | 97                |
| 20       | isobutyl  | 6.84±0.29                          | 1.2 (0.7-2.2) <sup>e</sup>            | 87                |
| 21       | CH <sub>2</sub> CF <sub>3</sub>   | 7.33±0.24                          | 5.0 (2.9-8.7)                         | 30                |
| 22       | CH <sub>2</sub> CH <sub>2</sub> F   | 6.95±0.12                          | 5.0 (2.9-8.7)                         | 68                |
| 23       |    | 6.86±0.18                          | >10                                   | 61                |
| 24       |  | 6.99±0.07                          | >10                                   | 37                |
| 25       |  | 6.63±0.12                          | >10                                   | 61                |
| 26       |  | 7.22±0.11                          | 1.2 (0.8-1.8) <sup>f</sup>            | 66                |
| 29       |  | 7.18±0.22                          | 1.2 (0.72-2.2)                        | 73                |

<sup>a</sup>Values are the mean ± SD of at least two experiments unless specified. <sup>b</sup>Wiga rats ( $n = 3$ ) were pretreated with test compound (sc) or solvent, and after 30 min, apomorphine (1.0 mg/kg, iv) induced stereotypy was scored every 5 min over the first hour after injection of apomorphine. <sup>c</sup>RLM data refer to the percentage of compound metabolized after incubation of the tested compound with rat microsomes for 15 min at 1  $\mu$ M concentration. <sup>d</sup>Not tested. <sup>e</sup>Doses of 0.63 mg/kg ( $n = 3$ ), 2.5 mg/kg ( $n = 8$ ), 5 mg/kg ( $n = 5$ ), and 10 mg/kg ( $n = 8$ ). <sup>f</sup> $n = 6$ .

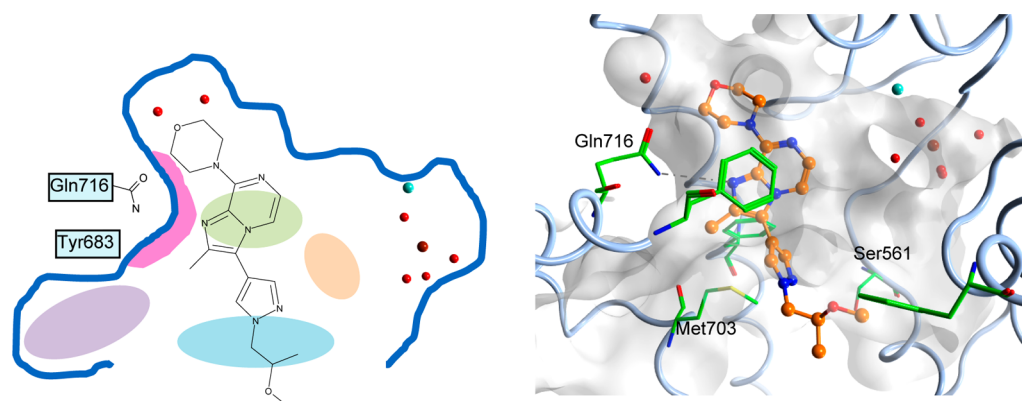
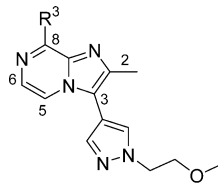


Figure 5. 2D and 3D representations of the cocystal structure of compound 26 (PDB 4BBX) bound to the PDE10A catalytic site.

water molecule than that in compound 36. Unfortunately, although compound 35 showed good in vitro activity and an

excellent in vivo potency in our apomorphine animal model (see Table 3), it was also accompanied by lethality in rats after

**Table 3.** PDE10A Inhibitory Activity of the Modifications at C8


| Compound | R <sup>3</sup>  | PDE10                              | APO                                   |
|----------|---|------------------------------------|---------------------------------------|
|          |   | pIC <sub>50</sub> ±SD <sup>a</sup> | ED <sub>50</sub> (mg/kg) <sup>b</sup> |
| 32       |  | 6.30±0.04                          | >10                                   |
| 35       |  | 6.46±0.10                          | 1.2 (0.7-2.2)                         |
| 36       |  | 6.25±0.10                          | n.t.                                  |

<sup>a</sup>Values are the mean ± SD of at least two experiments. <sup>b</sup>Wiga rats were pretreated with test compound (sc) or solvent, and after 30 min, apomorphine (1.0 mg/kg, iv) induced stereotypy was scored every 5 min over the first hour after injection of apomorphine. <sup>c</sup>The compound was not soluble and was tested orally as a suspension.

administration of a single dose of 40 mg/kg sc. As the reasons for this were unknown, this effect prohibited any further investigation.

On the basis of its promising in vivo activity in our apomorphine challenge model, compound **2** was selected for further in vivo evaluation in an additional model predictive of antipsychotic activity, the reversal of phencyclidine (PCP) induced hyperlocomotion in rats. This model is based on the evidence that the noncompetitive *N*-methyl-*D*-aspartate (NMDA) receptor antagonist PCP produces schizophrenia-like symptoms such as hallucinations and delusions in healthy subjects,<sup>29</sup> which preclinically correlates with an increase in motor activity in rodents. Compound **2** was able to revert PCP-induced hyperlocomotion in rats with an ED<sub>50</sub> comparable to that obtained for apomorphine antagonism. Finally, and to confirm target engagement of PDE10A in the brain, central occupancy of **2** was evaluated by displacement of [<sup>3</sup>H]MP-10.<sup>30</sup> The specific binding was determined as the difference between

[<sup>3</sup>H]MP-10 binding quantified in the striatum (a brain area showing a high density of PDE10A enzyme) and in the cortex (a brain area where PDE10A is virtually absent). Occupancy was calculated as the inhibition of specific [<sup>3</sup>H]MP-10 binding in drug-treated animals relative to vehicle-treated animals. As can be seen from the data in Table 4, there was a very good correlation between the ED<sub>50</sub> values for the inhibition of apomorphine-induced stereotypy, reversal of PCP-induced hyperlocomotion, and occupancy of PDE10 in rat brain, which together made us confident in the validity and utility of these paradigms for in vivo assessment of PDE10A inhibitory activity.

Comparison of the in vitro and in vivo data revealed that despite there being a >2 log units difference in in vitro PDE10A inhibition between the reference compound MP10 and **2**, this did not translate into similar differences in in vivo activity. A plausible explanation may be that the much lower plasma protein binding of compound **2** compared to MP10 (see Table 4) may account for a much higher free fraction of **2** in the brain. In fact, determination of the brain tissue binding for compound **2** and MP-10 revealed an excellent correlation between the bound fractions in plasma and in the brain, which appeared to support this hypothesis.

The preliminary characterization of compound **2** was completed with the evaluation of its pharmacokinetic profile in rats (Table 5). As seen from the data in Table 5, pharmacokinetic studies with compound **2** dosed at 10 mg/kg orally (po) and 2.5 mg/kg intravenously (iv) revealed a favorable profile with a high maximum concentration (C<sub>max</sub> = 1980 ng/mL) and exposure (AUC<sub>0–inf</sub> = 8487 (ng·h)/mL), an acceptable half-life (t<sub>1/2</sub> = 3.5 h), moderate clearance (Cl = 1.7 L h<sup>-1</sup> kg<sup>-1</sup>), and a good bioavailability (F<sub>abs</sub> = 52%). Finally, additional evaluation of **2** showed low cytochrome P450 (CYPs) enzyme (3A4, 2C9, 2D6, 1A2, 2C9) inhibition potential (IC<sub>50</sub> > 10 μM), minimal interaction with the hERG channel according to the binding assay (hERG pIC<sub>50</sub> < 5), and no effect in the Ames II genotoxicity assay.

In summary, starting from an HTS campaign, we identified the imidazo[1,2-*a*]pyrazine **1** as an interesting new PDE10A inhibitor hit. This compound showed good PDE10A inhibitory activity but lacked adequate selectivity versus other PDEs. Overlapping of compound **1** with other hits identified in the HTS campaign led us to the identification of the (methoxyethyl)pyrazole moiety as a good replacement for the trimethoxyphenyl group, leading to compound **8**. Systematic

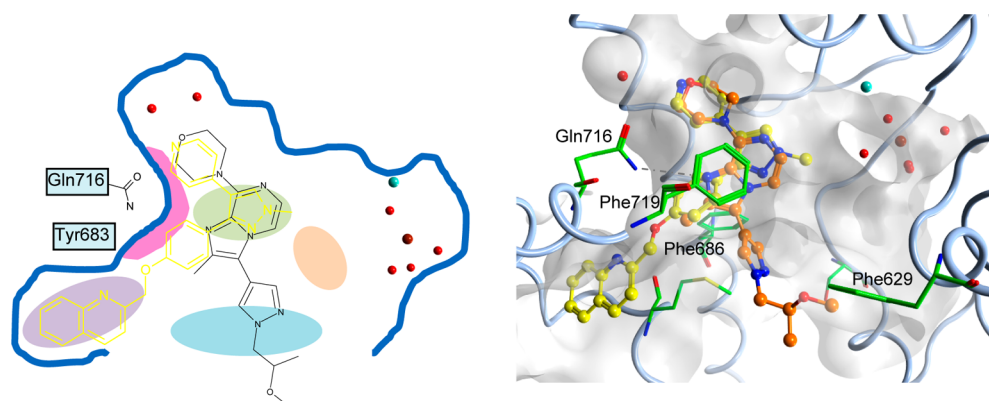


**Figure 6.** 2D and 3D representations of the cocrystal structure of **26** (orange, PDB code 4BBX) bound to the PDE10A catalytic site, superimposed with MP-10 from its cocrystal structure (yellow, PDB code 3HR1).

Table 4. In Vitro and in Vivo Profile of MP-10 and Compound 2

| compd | PDE10A pIC <sub>50</sub> ± SD <sup>a</sup> | apo ED <sub>50</sub> <sup>b</sup> (mg/kg) | PCP ED <sub>50</sub> <sup>c</sup> (mg/kg) | Occ ED <sub>50</sub> <sup>d</sup> (mg/kg) | rPPB bound <sup>e</sup> (%) | BTB bound <sup>f</sup> (%) |
|-------|--|---|---|---|-----------------------------|----------------------------|
| MP-10 | 9.19 ± 0.31                                | 0.67 (0.45–1.01)                          | 0.44 (0.36–0.55)                          | 1.58 (1.37–1.81)                          | 99.74                       | 99.8                       |
| 2     | 6.85 ± 0.14                                | 3.6 (2.8–4.4)                             | 5.0 (1.8–14)                              | 4.35 (2.90–6.52)                          | 73                          | 73                         |

<sup>a</sup>Values are the mean ± SD of at least three experiments. <sup>b</sup>Wiga rats ( $n = 5$ ) were pretreated with test compound (sc) or solvent, and after 30 min, apomorphine (1.0 mg/kg, iv) induced stereotypy was scored every 5 min over the first hour after injection of apomorphine. <sup>c</sup>Wiga rats ( $n = 3$ ) were pretreated with test compound (sc) or solvent. After 60 min, the rats were challenged with PCP (1.25 mg/kg, iv), and motor activity was measured over a period of 30 min starting immediately after the PCP challenge. <sup>d</sup>Dose–response experiments were performed to measure PDE10 occupancy 1 h after oral (po) administration. <sup>e</sup>Data refer to the percentage of compound bound to plasma proteins. <sup>f</sup>Data refer to the percentage of compound bound to brain tissue.

Table 5. Rat Pharmacokinetic Data of 2 (10 mg/kg po and 2.5 mg/kg iv)

| compd | C <sub>max</sub> (ng/mL) | AUC <sub>0–inf</sub> (10 mg/kg, po) [(ng·h)/mL] | t <sub>1/2</sub> (h) | F <sub>abs</sub> (%) | Cl (L h <sup>-1</sup> kg <sup>-1</sup> ) |
|-------|--------------------------|---|----------------------|----------------------|--|
| 2     | 1980                     | 8487  | 3.5                  | 52                   | 1.7                                      |

SAR studies from 8 resulted in the identification of compound 2, which combined good in vitro PDE10A activity with promising in vivo efficacy in various animal models predictive of antipsychotic efficacy (reversal of apomorphine-induced stereotypy and reversal of PCP-induced hyperlocomotion). Furthermore, target engagement in rat brain was confirmed by displacement of the selective PDE10A ligand [<sup>3</sup>H]MP-10 in the striatum. Finally, pharmacokinetic characterization revealed how compound 2 possessed a well-balanced overall profile. Taken together, these results suggest the imidazo[1,2-*a*]pyrazine series has promise as a novel series of PDE10A-selective inhibitors. Further evaluation of 2 and SAR refinement are under way and will be communicated in due course.

## EXPERIMENTAL SECTION

**General Procedures.** Unless otherwise noted, all reagents and solvents were obtained from commercial suppliers and used without further purification. Thin-layer chromatography (TLC) was carried out on silica gel 60 F254 plates (Merck). Flash column chromatography was performed on silica gel, particle size 60 Å, 230–400 mesh (Merck), under standard techniques. Microwave-assisted reactions were performed in a single-mode reactor (Biotage Initiator Sixty microwave reactor (Biotage)) or in a multimode reactor (MicroSYNTH Labstation (Milestone, Inc.)). Nuclear magnetic resonance (NMR) spectra were recorded with either a Bruker DPX-400 or a Bruker AV-500 spectrometer (Bruker AG) with standard pulse sequences operating at 400 and 500 MHz, respectively, using CDCl<sub>3</sub> and DMSO-*d*<sub>6</sub> as solvents. Chemical shifts ( $\delta$ ) are reported in parts per million downfield from tetramethylsilane ( $\delta = 0$ ). Coupling constants are reported in hertz. Splitting patterns are defined by s (singlet), d (doublet), dd (doublet of doublets), t (triplet), q (quartet), and m (multiplet). The purities of all new compounds were determined by analytical reversed-phase (RP) HPLC or UPLC coupled to a mass spectrometry detector using the area percentage method on the UV trace and were found to be  $\geq 95\%$  unless otherwise specified. The HPLC or UPLC measurement was performed using either an HP 1100 (Agilent Technologies) system or an Acquity system (Waters) comprising a pump (quaternary or binary) with a degasser, an autosampler, a column oven, a diode-array detector (DAD), and a column as specified in the respective methods. The MS detector (SQD, TOF, MSD, ZQ, platform, or QTOF) was configured with an electrospray ionization source. Nitrogen was used as the nebulizer gas. Data acquisition was performed with MassLynx-Openlynx software or Chemstation-Agilent Data Browser software. Detailed information about the different LC–MS methods employed can be found in the Supporting Information. Melting point (mp) values are peak values and were obtained with experimental uncertainties that are commonly associated with this analytical method. Melting points were determined in open capillary tubes either on a Mettler FP62 or on an FP 81HT/FP90 apparatus with a

temperature gradient of 10 °C/min. The maximum temperature was 300 °C.

**(3-Chloropyrazin-2-yl)amine (4).** A mixture of 2,3-dichloropyrazine (5 g, 33.6 mmol) and ammonium hydroxide solution (28% in water, 25 mL) was stirred at 100 °C in a Parr vessel for 24 h. Then the cooled reaction was diluted with water and filtered. The solid was washed with water and dried in vacuo, affording 3.93 g (90%) of 4 as a white solid. MS:  $m/z$  130 [M + H]<sup>+</sup>.  $t_R = 0.4$  min. <sup>1</sup>H NMR (500 MHz, DMSO-*d*<sub>6</sub>):  $\delta$  (ppm) 6.78 (br s, 2 H), 7.58 (d,  $J = 2.6$  Hz, 1 H), 7.96 (d,  $J = 2.6$  Hz, 1 H). Mp: 169.4–170.1 °C.

**8-Chloroimidazo[1,2-*a*]pyrazine (5a).** Bromoacetaldehyde diethyl acetal (17.4 mL, 115.8 mmol) was added dropwise to a 48% aqueous solution of HBr (4.45 mL, 38.6 mmol) at room temperature. The mixture was stirred at reflux temperature for 2 h and then poured onto a suspension of sodium hydrogen carbonate (74.5 g, 0.88 mol) in 2-propanol (220 mL). The mixture was stirred for a further 30 min and then filtered off. 4 (5 g, 38.6 mmol) was added to the filtrate, and the mixture was stirred at 85 °C for 4 h. The solvent was evaporated in vacuo and the crude product suspended in a saturated solution of sodium hydrogen carbonate and extracted with DCM. The organic layer was separated, dried (Na<sub>2</sub>SO<sub>4</sub>), and filtered and the solvent evaporated in vacuo. The crude product was precipitated from diethyl ether to yield 5a (4.1 g, 70%) as a brown solid which was used in the next step without further purification. MS:  $m/z$  154 [M + H]<sup>+</sup>.  $t_R = 0.32$  min. <sup>1</sup>H NMR (500 MHz, CDCl<sub>3</sub>):  $\delta$  (ppm) 7.70 (d,  $J = 4.6$  Hz, 1 H), 7.78 (d,  $J = 0.6$  Hz, 1 H), 7.85 (br s, 1 H), 8.07 (d,  $J = 4.6$  Hz, 1 H).

**8-Chloro-2-methylimidazo[1,2-*a*]pyrazine (5b).** A mixture of chloroacetone (120 mL, 1505 mmol) and 4 (48.69 g, 376 mmol) was stirred at 90 °C for 18 h. The solvent was removed and the residue dissolved in DCM and washed with a saturated solution of sodium hydrogen carbonate. The organic layer was separated, dried (Na<sub>2</sub>SO<sub>4</sub>), and filtered, and the solvents were evaporated in vacuo. The resulting residue was precipitated from diethyl ether and filtered to yield 5b as a pale yellow solid (43.2 g, 68.5%). MS:  $m/z$  168 [M + H]<sup>+</sup>.  $t_R = 0.49$  min. <sup>1</sup>H NMR (400 MHz, CDCl<sub>3</sub>):  $\delta$  (ppm) 2.55 (s, 3 H), 7.54 (s, 1 H), 7.63 (d,  $J = 4.6$  Hz, 1 H), 7.96 (d,  $J = 4.6$  Hz, 1 H). Mp: 133.5–138.6 °C.

**8-Chloro-2-ethylimidazo[1,2-*a*]pyrazine (5c).** Compound 5c was prepared starting from 4 and 1-bromobutan-2-one similarly to the preparation of 5b. Precipitation from diethyl ether yielded 5c (100%) as a pale brown solid. <sup>1</sup>H NMR (400 MHz, CDCl<sub>3</sub>):  $\delta$  (ppm) 1.37 (t,  $J = 7.6$  Hz, 3 H), 2.92 (qd,  $J = 7.6, 0.7$  Hz, 2 H), 7.55 (br s, 1 H), 7.63 (d,  $J = 4.6$  Hz, 1 H), 7.98 (d,  $J = 4.6$  Hz, 1 H).

**8-Chloro-2-cyclopropylimidazo[1,2-*a*]pyrazine (5d).** 2-Bromo-1-cyclopropylethanone<sup>31</sup> (64.5 mL, 617.5 mmol) was added to a solution of 4 (40.0 g, 308.8 mmol) in ACN (500 mL), and the reaction mixture was stirred at 90 °C for 18 h. The solvent was removed and the residue dissolved in DCM and washed with a saturated solution of sodium hydrogen carbonate. The organic layer was separated, dried (Na<sub>2</sub>SO<sub>4</sub>), and filtered, and the solvents were evaporated in vacuo to yield 5d as a pale yellow solid (22.5 g, 38%).

MS:  $m/z$  194  $[M + H]^+$ .  $t_R = 3.81$  min.  $^1H$  NMR (400 MHz,  $CDCl_3$ ):  $\delta$  (ppm) 0.91–1.02 (m, 2 H), 1.02–1.11 (m, 2 H), 2.07–2.19 (m, 1 H), 7.49 (s, 1 H), 7.61 (d,  $J = 4.3$  Hz, 1 H), 7.93 (d,  $J = 4.5$  Hz, 1 H). Mp: 63.5–66.3 °C.

**8-Chloro-2-(trifluoromethyl)imidazo[1,2-*a*]pyrazine (5e).** *Step 1: Synthesis of 8-Hydroxy-2-(trifluoromethyl)imidazo[1,2-*a*]pyrazine.* A mixture of **4** (0.50 g, 3.86 mmol) and 1-chloro-3,3,3-trifluoroacetone (4 mL, 0.027 mmol) was stirred at 100 °C for 16 h. The mixture was partitioned between DCM and a saturated solution of sodium hydrogen carbonate. The organic layer was separated, dried ( $Na_2SO_4$ ), and filtered, and the solvents were evaporated in vacuo to yield 8-hydroxy-2-(trifluoromethyl)imidazo[1,2-*a*]pyrazine (0.31 g, 39%) as a pale brown solid which was used in the next step without further purification. MS:  $m/z$  204  $[M + H]^+$ .  $t_R = 0.46$  min.  $^1H$  NMR (500 MHz,  $DMSO-d_6$ ):  $\delta$  (ppm) 6.99 (t,  $J = 5.6$  Hz, 1 H), 7.51 (d,  $J = 4.6$  Hz, 1 H), 8.42 (s, 1 H), 11.46 (br s, 1 H).

*Step 2: Synthesis of 5e.* A mixture of 8-hydroxy-2-(trifluoromethyl)imidazo[1,2-*a*]pyrazine (0.169 g, 0.83 mmol) and *N,N*-dimethylaniline (0.06 mL, 0.006 mmol) in phosphorus oxychloride (0.60 mL, 1 mmol) was stirred at 90 °C for 4 h. The mixture was allowed to cool to room temperature, and then the red solid obtained was poured onto crushed ice and extracted with DCM. The organic layer was separated, dried ( $Na_2SO_4$ ), and filtered, and the solvents were evaporated in vacuo to yield **5e** (0.182 g, 99%) as a brown solid which was used in the next step without further purification. MS:  $m/z$  222  $[M + H]^+$ .  $t_R = 1.65$  min.  $^1H$  NMR (400 MHz,  $CDCl_3$ ):  $\delta$  (ppm) 7.82 (d,  $J = 4.6$  Hz, 1 H), 8.08 (s, 1 H), 8.09 (d,  $J = 4.6$  Hz, 1 H).

**8-Chloroimidazo[1,2-*a*]pyrazine-2-carboxylic Acid Ethyl Ester Hydrobromide (5f).** A mixture of **4** (2.50 g, 19.3 mmol) and ethyl bromopyruvate (2.9 mL, 23.16 mmol) in 1,2-dimethoxyethane (60 mL) was stirred at room temperature for 2.5 h. Then the reaction mixture was cooled to 0 °C and stirred for a further 30 min. The white solid formed was filtered off, washed with diethyl ether, suspended in EtOH, and stirred at room temperature for a further 20 h. The solvent was evaporated in vacuo and the crude product precipitated from DCM to yield **5f** (4.0 g, 92%) as a white solid (HBr) which was used in the next step without further purification. MS:  $m/z$  226  $[M + H]^+$ .  $t_R = 3.08$  min.  $^1H$  NMR (500 MHz,  $CDCl_3$ ):  $\delta$  (ppm) 1.45 (t,  $J = 7.2$  Hz, 3 H), 4.50 (q,  $J = 7.2$  Hz, 2 H), 7.77 (d,  $J = 4.6$  Hz, 1 H), 8.08 (d,  $J = 4.6$  Hz, 1 H), 8.33 (s, 1 H).

**3-Bromo-8-chloroimidazo[1,2-*a*]pyrazine (6a).** NBS (2.0 g, 11.6 mmol) was added to a stirred solution of **5a** (1.78 g, 11.58 mmol) in DCM (50 mL). The mixture was stirred at room temperature for 2 h, then diluted with further DCM, and washed with a saturated solution of sodium carbonate. The organic layer was separated, dried ( $Na_2SO_4$ ), and filtered and the solvent evaporated in vacuo to yield **6a** (5.89 g, 99%) as a white solid which was used in the next step without further purification.

**3-Bromo-8-chloro-2-methylimidazo[1,2-*a*]pyrazine (6b).** **6b** was prepared according to a protocol analogous to that for compound **6a** from **5b**. Precipitation from diethyl ether yielded **6b** as a white solid (99%) which was used in the next step without further purification. MS:  $m/z$  246  $[M + H]^+$ .  $t_R = 1.21$  min.  $^1H$  NMR (300 MHz,  $DMSO-d_6$ ):  $\delta$  (ppm) 2.43 (s, 3 H), 7.81 (d,  $J = 4.5$  Hz, 1 H), 8.38 (d,  $J = 4.5$  Hz, 1 H).

**3-Bromo-8-chloro-2-ethylimidazo[1,2-*a*]pyrazine (6c).** **6c** was prepared according to a protocol analogous to that for compound **6a** from **5c**. Precipitation from diethyl ether yielded **6c** as a white solid (100%) which was used in the next step without further purification.  $^1H$  NMR (400 MHz,  $CDCl_3$ ):  $\delta$  (ppm) 1.37 (t,  $J = 7.6$  Hz, 3 H), 2.91 (q,  $J = 7.6$  Hz, 2 H), 7.77 (d,  $J = 4.6$  Hz, 1 H), 7.97 (d,  $J = 4.4$  Hz, 1 H).

**3-Bromo-8-chloro-2-cyclopropylimidazo[1,2-*a*]pyrazine (6d).** **6d** was prepared according to a protocol analogous to that for compound **6a** from **5d**. Precipitation from diethyl ether yielded **6d** as a white solid (73%) which was used as such in the next reaction. MS:  $m/z$  272  $[M + H]^+$ .  $t_R = 2.92$  min.

**3-Bromo-8-chloro-2-(trifluoromethyl)imidazo[1,2-*a*]pyrazine (6e).** **6e** was prepared according to a protocol analogous to

that for compound **6a** from **5e**. Flash column chromatography (silica; AcOEt in heptane, 20/80) yielded **6e** as a white solid (73%). MS:  $m/z$  344  $[M + H]^+$ .  $t_R = 2.83$  min.  $^1H$  NMR (400 MHz,  $CDCl_3$ ):  $\delta$  (ppm) 7.93 (t,  $J = 4.4$  Hz, 1 H) 8.11 (t,  $J = 4.4$  Hz, 1 H).

**3-Bromo-8-chloroimidazo[1,2-*a*]pyrazine-2-carboxylic Acid Ethyl Ester (6f).** **6f** was prepared according to a protocol analogous to that for compound **6a** from **5f**. Precipitation from diethyl ether yielded **6f** as a white solid (83%) which was used in the next step without further purification. MS:  $m/z$  304  $[M + H]^+$ .  $t_R = 0.91$  min.  $^1H$  NMR (500 MHz,  $CDCl_3$ ):  $\delta$  (ppm) 1.48 (t,  $J = 7.1$  Hz, 3 H), 4.53 (q,  $J = 7.0$  Hz, 2 H), 7.88 (d,  $J = 4.6$  Hz, 1 H), 8.12 (d,  $J = 4.6$  Hz, 1 H).

**3-Bromo-8-morpholin-4-ylimidazo[1,2-*a*]pyrazine (7a).** Morpholine (2.0 mL, 23.2 mmol) was added to a stirred solution of **6a** (5.9 g, 11.6 mmol) and DIPEA (1.93 mL, 13.9 mmol) in ACN (54 mL). The mixture was stirred at 80 °C for 7 h, and then the solvent was evaporated in vacuo. The crude product was dissolved in DCM and washed with a saturated solution of sodium carbonate. The organic layer was separated, dried ( $Na_2SO_4$ ), and filtered, and the solvents were evaporated in vacuo. The crude product was purified by flash column chromatography (silica; AcOEt in DCM, 10/90). The desired fractions were collected, the solvent was evaporated in vacuo, and the impure product was precipitated from diethyl ether to yield **7a** (2.79 g, 85%) as a white solid. MS:  $m/z$  283  $[M + H]^+$ .  $t_R = 2.70$  min.

**3-Bromo-2-methyl-8-morpholin-4-ylimidazo[1,2-*a*]pyrazine (7b).** **7b** was prepared according to a protocol analogous to that for compound **7a** from **6b**. Flash column chromatography (silica; AcOEt in DCM, 50/50) yielded **7b** as a white solid (71%).  $^1H$  NMR (400 MHz,  $CDCl_3$ ):  $\delta$  (ppm) 2.44 (s, 3 H), 3.89 (br t,  $J = 4.8, 4.8$  Hz, 4 H), 4.26 (br t,  $J = 4.5, 4.5$  Hz, 4 H), 7.47 (br s, 2 H). Mp: 159.3–159.8 °C.

**3-Bromo-2-ethyl-8-morpholin-4-ylimidazo[1,2-*a*]pyrazine (7c).** **7c** was prepared according to a protocol analogous to that for compound **7a** from **6c**. Trituration with ACN yielded **7c** as a white solid (83%). MS:  $m/z$  311  $[M + H]^+$ .  $t_R = 2.28$  min.  $^1H$  NMR (400 MHz,  $CDCl_3$ ):  $\delta$  (ppm) 1.31 (t,  $J = 7.5$  Hz, 3 H), 2.77 (q,  $J = 7.5$  Hz, 2 H), 3.84–3.88 (m, 4 H), 4.23–4.27 (m, 4 H), 7.43 (d,  $J = 4.4$  Hz, 1 H), 7.46 (d,  $J = 4.6$  Hz, 1 H).

**3-Bromo-2-cyclopropyl-8-morpholin-4-ylimidazo[1,2-*a*]pyrazine (7d).** **7d** was prepared according to a protocol analogous to that for compound **7a** from **6d**. Flash column chromatography (silica; 7 M solution of ammonia in MeOH in DCM, 1/99 to 2/98) yielded **7d** as a pale brown solid (48%). MS:  $m/z$  323  $[M + H]^+$ .  $t_R = 2.48$  min.  $^1H$  NMR (500 MHz,  $CDCl_3$ ):  $\delta$  (ppm) 0.96–1.05 (m, 4 H) 2.01–2.07 (m, 1 H) 3.82–3.85 (m, 4 H) 4.18–4.22 (m, 4 H) 7.41 (d,  $J = 4.33$  Hz, 1 H) 7.44 (d,  $J = 4.33$  Hz, 1 H).

**3-Bromo-8-morpholin-4-yl-2-(trifluoromethyl)imidazo[1,2-*a*]pyrazine (7e).** **7e** was prepared according to a protocol analogous to that for compound **7a** from **6e**. Flash column chromatography (silica; AcOEt in heptane, 10/90) yielded **7e** as a white solid (99%).  $^1H$  NMR (400 MHz,  $CDCl_3$ ):  $\delta$  (ppm) 3.85 (t,  $J = 4.9$  Hz, 4 H), 4.29 (t,  $J = 4.6$  Hz, 4 H), 7.51 (d,  $J = 4.6$  Hz, 1 H), 7.55 (d,  $J = 4.6$  Hz, 1 H).

**3-Bromo-8-morpholin-4-ylimidazo[1,2-*a*]pyrazine-2-carboxylic Acid Ethyl Ester (7f).** **7f** was prepared according to a protocol analogous to that for compound **7a** from **6f**. Flash column chromatography (silica; AcOEt in heptane, 50/50) yielded **7f** as a white solid (99%). MS:  $m/z$  355  $[M + H]^+$ .  $t_R = 1.14$  min.  $^1H$  NMR (400 MHz,  $CDCl_3$ ):  $\delta$  (ppm) 1.45 (t,  $J = 7.1$  Hz, 3 H), 3.83–3.89 (m, 4 H), 4.26–4.37 (m, 4 H), 4.46 (q,  $J = 7.0$  Hz, 2 H), 7.51 (d,  $J = 4.6$  Hz, 1 H), 7.55 (d,  $J = 4.6$  Hz, 1 H).

**(3-Morpholin-4-ylpyrazin-2-yl)amine (15).** A mixture of morpholine (37 mL, 433 mmol) and **4** (10.2 g, 79 mmol) was stirred at 120 °C for 16 h. The excess morpholine was evaporated in vacuo, and the crude product was washed with a 5% solution of ammonium hydroxide. The organic layer was separated, dried ( $MgSO_4$ ), and filtered and the solvent evaporated in vacuo to yield **14** (12 g, 84%) as a white solid. MS:  $m/z$  181  $[M + H]^+$ .  $t_R = 2.81$  min.  $^1H$  NMR (500 MHz,  $CDCl_3$ ):  $\delta$  (ppm) 3.12–3.21 (m, 4 H), 3.81–3.91 (m, 4 H), 4.63 (br s, 2 H), 7.67 (d,  $J = 2.6$  Hz, 1 H), 7.70 (d,  $J = 2.6$  Hz, 1 H). Mp: 158.1–160.4 °C.

**2-Methoxy-8-morpholin-4-ylimidazo[1,2-*a*]pyrazine (16).**

**Step 1: Synthesis of 8-Morpholin-4-ylimidazo[1,2-*a*]pyrazin-2-ol.** Bromoacetic acid (5.55 g, 39.9 mmol) was added to a stirred solution of **15** (6.0 g, 33.3 mmol) in 2-propanol (48 mL). The mixture was stirred at 90 °C for 16 h, and the solid formed was filtered off to yield 8-morpholin-4-ylimidazo[1,2-*a*]pyrazin-2-ol (7.7 g, 77%) as a pale brown solid. MS:  $m/z$  221  $[M + H]^+$ .  $t_R = 0.27$  min.  $^1H$  NMR (400 MHz, DMSO- $d_6$ ):  $\delta$  (ppm) 3.51 (br s, 1 H), 3.82 (t,  $J = 4.9$  Hz, 4 H), 4.20 (t,  $J = 4.2$  Hz, 4 H), 7.34 (d,  $J = 5.3$  Hz, 1 H), 7.45 (s, 1 H), 8.01 (d,  $J = 5.1$  Hz, 1 H), 11.06 (br s, 1 H).

**Step 2: Synthesis of 16.** Cesium carbonate (12.98 g, 39.85 mmol) was added to a stirred solution of iodomethane (1.24 mL, 19.92 mmol) and 8-morpholin-4-ylimidazo[1,2-*a*]pyrazin-2-ol (4.0 g, 13.28 mmol) in DMF (150 mL). The mixture was stirred at room temperature for 1 h, and then the solvent was evaporated in vacuo. The crude product was purified by flash column chromatography (silica; AcOEt in heptane, 30/70). The desired fractions were collected, and the solvent was evaporated in vacuo to yield **16** (1.38 g, 39%) as a white solid. MS:  $m/z$  235  $[M + H]^+$ .  $t_R = 0.97$  min.

**3-Bromo-2-methoxy-8-morpholin-4-ylimidazo[1,2-*a*]pyrazine (7g).** **7g** was prepared according to a protocol analogous to that for compound **6a** from **16**. Flash column chromatography (silica; AcOEt in DCM, 10/90) yielded **7g** as a white solid (86%). MS:  $m/z$  313  $[M + H]^+$ .  $t_R = 1.92$  min.  $^1H$  NMR (500 MHz, CDCl<sub>3</sub>):  $\delta$  (ppm) 3.83–3.90 (m, 4 H), 4.07 (s, 3 H), 4.14–4.20 (m, 4 H), 7.44 (d,  $J = 4.3$  Hz, 1 H), 7.51 (d,  $J = 4.3$  Hz, 1 H).

**1-(2-Methoxyethyl)-4-(4,4,5,5-tetramethyl[1,3,2]-dioxaborolan-2-yl)-1H-pyrazole (12a).** 2-Chloroethyl methyl ether (3.06 mL, 33.5 mmol) was added to a stirred solution of 4-(4,4,5,5-tetramethyl[1,3,2]dioxaborolan-2-yl)-1H-pyrazole (**12**) (5.0 g, 25.77 mmol) and cesium carbonate (12.59 g, 38.65 mmol) in DMF (27 mL). The mixture was stirred at 160 °C for 30 min under microwave irradiation, and then the solvent was evaporated in vacuo. The crude product was purified by flash column chromatography (silica; 7 M solution of ammonia in MeOH in DCM, 2/98). The desired fractions were collected, and the solvent was evaporated in vacuo to yield **12a** (6.5 g, 100%) as a pale yellow oil.  $^1H$  NMR (500 MHz, CDCl<sub>3</sub>):  $\delta$  (ppm) 1.32 (s, 12 H), 3.32 (s, 3 H), 3.75 (t,  $J = 5.3$  Hz, 2 H), 4.30 (t,  $J = 5.3$  Hz, 2 H), 7.76 (s, 1 H), 7.79 (s, 1 H).

**1-(Cyclopropylmethyl)-4-(4,4,5,5-tetramethyl[1,3,2]-dioxaborolan-2-yl)-1H-pyrazole (12b).** **12** (5 g, 25.8 mmol), (bromomethyl)cyclopropane (10 mL, 103.1 mmol), and potassium carbonate (10.69 g, 77.3 mmol) in acetone (90 mL) were stirred at 65 °C for 3 days. The solvent was evaporated in vacuo. The residue was partitioned between DCM and water. The organic layer was separated, dried (Na<sub>2</sub>SO<sub>4</sub>), and filtered, and the solvents were evaporated in vacuo. The crude product was purified by flash column chromatography (silica; 7 M solution of ammonia in MeOH in DCM, 1/99). The desired fractions were collected, and the solvent was evaporated in vacuo to yield **12b** (5.7 g, 89%) as a yellow solid. Mp: 102.7–109.3 °C.

**1-Isopropyl-4-(4,4,5,5-tetramethyl[1,3,2]dioxaborolan-2-yl)-1H-pyrazole (12c).** **12c** was prepared according to a protocol analogous to that for **12a** from 2-bromopropane and **12**. Flash column chromatography (silica; 7 M solution of ammonia in MeOH in DCM, 1/99) yielded **12c** as a pale green oil (50%). MS:  $m/z$  237  $[M + H]^+$ .  $t_R = 3.82$  min.

**4-(4,4,5,5-Tetramethyl[1,3,2]dioxaborolan-2-yl)-1-(2,2,2-trifluoroethyl)-1H-pyrazole (12e).** **12c** was prepared according to a protocol analogous to that for **12a** from 2,2,2-trifluoroethyl trifluoromethanesulfonate and **12** to yield **12e** as an oil (70%).

**4-(4,4,5,5-Tetramethyl[1,3,2]dioxaborolan-2-yl)-1-(2-fluoroethyl)-1H-pyrazole (12f).** **12f** was prepared according to a protocol analogous to that for **12a** from 1-bromo-2-fluoroethane and **12** to yield **12f** as an oil (40%).

**1-(2-Chlorobenzyl)-4-(4,4,5,5-tetramethyl[1,3,2]-dioxaborolan-2-yl)-1H-pyrazole (12g).** **Step 1: Synthesis of 1-(2-Chlorobenzyl)-4-iodo-1H-pyrazole.** Cesium carbonate (50 g, 153 mmol) was added to a mixture of 2-chlorobenzyl chloride (18 g, 111 mmol) and 4-iodopyrazole (20 g, 103 mmol) in ACN (250 mL), and the mixture was refluxed for 18 h. The solid was filtered and washed

with ACN. The filtrate was concentrated to dryness, and the crude product was purified by flash column chromatography (silica; AcOEt in petroleum ether, 1/10 to 1/5) to yield 1-(2-chlorobenzyl)-4-iodo-1H-pyrazole (30 g, 92%).

**Step 2: Synthesis of 12g.** [1,1'-Bis(diphenylphosphino)ferrocene]-dichloropalladium(II) (1 g, 1.4 mmol) was added to a stirred solution of 1-(2-chlorobenzyl)-4-iodo-1H-pyrazole (18.3 g, 58 mmol), 4,4,4',4',5,5,5',5'-octamethyl-2,2'-bi-1,3,2-dioxaborolane (25 g, 98 mmol), and potassium acetate (19.5 g, 198 mmol) in DMF (400 mL). The mixture was stirred at 80 °C for 16 h. The mixture was filtered through a pad of diatomaceous earth, and the solvent was evaporated in vacuo. The crude product was purified by flash column chromatography (silica; AcOEt in petroleum ether, 1/10) to yield **12g** (5.5 g, 30%).  $^1H$  NMR (500 MHz, CDCl<sub>3</sub>):  $\delta$  (ppm) 1.31 (s, 12 H), 5.44 (s, 2 H), 7.05 (dd,  $J = 7.5, 1.7$  Hz, 1 H), 7.18–7.25 (m, 1 H), 7.24–7.28 (m, 1 H), 7.39 (dd,  $J = 7.8, 1.4$  Hz, 1 H), 7.73 (s, 1 H), 7.84 (s, 1 H).

**4-[[4-(4,4,5,5-Tetramethyl[1,3,2]dioxaborolan-2-yl)pyrazol-1-yl]methyl]pyridine (12h).** **12h** was prepared according to a protocol analogous to that for **12a** from 4-(chloromethyl)pyridine hydrochloride and **12**. Flash column chromatography (silica; 7 M solution of ammonia in MeOH in DCM, 2/98) yielded **12h** as a yellow oil (11% purity, 62%) which was used in the next step without any further purification.

**3-[[4-(4,4,5,5-Tetramethyl[1,3,2]dioxaborolan-2-yl)pyrazol-1-yl]methyl]isoquinoline (12i).** **12i** was prepared according to a protocol analogous to that for **12a** from 2-(chloromethyl)quinoline monohydrochloride and **12**. Flash column chromatography (silica; 7 M solution of ammonia in MeOH in DCM, 2/98; then AcOEt in heptane, 60/40) yielded **12i** as an oil (7%).

**1-(2-Methoxy-2(S)-methylethyl)-4-(4,4,5,5-tetramethyl[1,3,2]dioxaborolan-2-yl)-1H-pyrazole (12j).** **Step 1: Synthesis of Toluene-4-sulfonic Acid 2-Methoxy-2(R)-methylethyl Ester.** A mixture of (S)-(+)-2-methoxypropanol (500 mg, 5.55 mmol), *p*-toluenesulfonyl chloride (1.59 g, 8.3 mmol), and triethylamine (1.54 mL, 11.1 mmol) in DCM (10 mL) was stirred at rt for 2 h. The mixture was washed with a saturated solution of Na<sub>2</sub>CO<sub>3</sub>. The organic layer was separated and dried (Na<sub>2</sub>SO<sub>4</sub>). The solvent was evaporated in vacuo to yield intermediate toluene-4-sulfonic acid 2-methoxy-2(R)-methylethyl ester (1.3 g, 95%) as an oil which was used in the next step without further purification. MS:  $m/z$  245  $[M + H]^+$ .  $t_R = 2.81$  min.  $^1H$  NMR (500 MHz, CDCl<sub>3</sub>):  $\delta$  (ppm) 1.28 (d,  $J = 6.6$  Hz, 3 H), 2.45 (s, 3 H), 3.25 (s, 3 H), 3.36 (dd,  $J = 10.7, 4.3$  Hz, 1 H), 3.42 (dd,  $J = 11.0, 5.8$  Hz, 1 H), 4.71 (dq,  $J = 6.4, 6.2, 6.2, 4.6$  Hz, 1 H), 7.33 (d,  $J = 8.1$  Hz, 2 H), 7.81 (d,  $J = 8.1$  Hz, 2 H).

**Step 2: Synthesis of 12j.** **12j** was prepared according to a protocol analogous to that for **12a** from toluene-4-sulfonic acid 2-methoxy-2(R)-methylethyl ester and **12**. Flash column chromatography (silica; AcOEt in heptane, 0/100 to 20/80) yielded **12j** as a yellow oil (78%).

**2-Methyl-3-[1-(2-methoxyethyl)-1H-pyrazol-4-yl]-8-morpholin-4-ylimidazo[1,2-*a*]pyrazine (2).** Palladium(II) acetate (0.005 g, 0.023 mmol) was added to a stirred solution of **7b** (0.1 g, 0.33 mmol), **12a** (0.127 g, 0.50 mmol), and triphenylphosphine (0.009 g, 0.034 mmol) in a mixture of 1,4-dioxane (3.0 mL) and potassium carbonate (0.84 mg, 1.26 mmol). The mixture was stirred at 80 °C for 8 h, and then the solvents were evaporated in vacuo. The crude product was partitioned between water and DCM, the organic layer was separated, dried (Na<sub>2</sub>SO<sub>4</sub>), and filtered, and the solvents were evaporated in vacuo. The crude product was purified by flash column chromatography (silica; 7 M solution of ammonia in MeOH in DCM, 2/98). The desired fractions were collected, and the solvent was evaporated in vacuo to yield **2** (0.098 g, 85%) as a white solid. UPLC/ESI-HRMS:  $m/z$  for C<sub>17</sub>H<sub>24</sub>N<sub>6</sub>O<sub>2</sub> (M + H)<sup>+</sup> calcd 343.1882, found 343.1898 (4.7 ppm).  $t_R = 1.30$  min.  $^1H$  NMR (500 MHz, DMSO- $d_6$ ):  $\delta$  (ppm) 2.39 (s, 3 H), 3.27 (s, 3 H), 3.75 (t,  $J = 5.2$  Hz, 4 H), 3.77 (t,  $J = 5.2$  Hz, 2 H), 4.15 (t,  $J = 4.9$  Hz, 4 H), 4.37 (t,  $J = 5.5$  Hz, 2 H), 7.38 (d,  $J = 4.6$  Hz, 1 H), 7.68 (d,  $J = 4.6$  Hz, 1 H), 7.82 (s, 1 H), 8.17 (s, 1 H). Mp: 100.1 °C.

**3-[1-(2-Methoxyethyl)-1H-pyrazol-4-yl]-8-morpholin-4-ylimidazo[1,2-*a*]pyrazine (8).** **8** was prepared according to a

protocol analogous to that for compound **2** from **7a** and **12a**. Flash column chromatography (7 M solution of ammonia in MeOH in DCM, 2/98) and reversed-phase HPLC yielded compound **8** as a white solid (85%). UPLC/ESI-HRMS:  $m/z$  for  $C_{16}H_{21}N_6O_2$  ( $M + H$ )<sup>+</sup> calcd 329.1726, found 329.1729 (0.9 ppm).  $t_R = 1.20$  min. <sup>1</sup>H NMR (500 MHz, DMSO- $d_6$ ):  $\delta$  (ppm) 3.26 (s, 3 H), 3.70–3.81 (m, 6 H), 4.19 (t,  $J = 4.6$  Hz, 4 H), 4.35 (t,  $J = 5.3$  Hz, 2 H), 7.45 (d,  $J = 4.6$  Hz, 1 H), 7.72 (s, 1 H), 7.87 (d,  $J = 4.6$  Hz, 1 H), 7.94 (s, 1 H), 8.31 (s, 1 H).

**2-Ethyl-3-[1-(2-methoxyethyl)-1H-pyrazol-4-yl]-8-morpholin-4-ylimidazo[1,2-a]pyrazine (9)**. **9** was prepared according to a protocol analogous to that for compound **2** from **7c** and **12a**. Flash column chromatography (silica; 7 M solution of ammonia in MeOH in DCM, 0/100 to 2/98) and reversed-phase HPLC yielded compound **9** as a white solid (28%). UPLC/ESI-HRMS:  $m/z$  for  $C_{18}H_{25}N_6O_2$  ( $M + H$ )<sup>+</sup> calcd 357.2039, found 357.2040 (0.3 ppm).  $t_R = 1.57$  min. <sup>1</sup>H NMR (400 MHz, DMSO- $d_6$ ):  $\delta$  (ppm) 1.22 (t,  $J = 7.5$  Hz, 3 H), 2.72 (q,  $J = 7.6$  Hz, 2 H), 3.26 (s, 3 H), 3.70–3.81 (m, 6 H), 4.16 (br t,  $J = 4.9$  Hz, 4 H), 4.36 (t,  $J = 5.3$  Hz, 2 H), 7.37 (d,  $J = 4.6$  Hz, 1 H), 7.63 (d,  $J = 4.4$  Hz, 1 H), 7.77 (d,  $J = 0.7$  Hz, 1 H), 8.14 (d,  $J = 0.7$  Hz, 1 H).

**2-Cyclopropyl-3-[1-(2-methoxyethyl)-1H-pyrazol-4-yl]-8-morpholin-4-ylimidazo[1,2-a]pyrazine (10)**. **10** was prepared according to a protocol analogous to that for **2** from **7d** and **12a**. Flash column chromatography (silica; AcOEt) yielded **10** as a gray solid (87%). UPLC/ESI-HRMS:  $m/z$  for  $C_{19}H_{25}N_6O_2$  ( $M + H$ )<sup>+</sup> calcd 369.2039, found 369.2039 (0.0 ppm).  $t_R = 1.78$  min. <sup>1</sup>H NMR (500 MHz, DMSO- $d_6$ ):  $\delta$  (ppm) 0.83–0.99 (m, 4 H), 2.00–2.09 (m, 1 H), 3.26 (s, 3 H), 3.72 (t,  $J = 4.9$  Hz, 4 H), 3.77 (t,  $J = 5.3$  Hz, 2 H), 4.11 (t,  $J = 4.3$  Hz, 4 H), 4.37 (t,  $J = 5.5$  Hz, 2 H), 7.36 (d,  $J = 4.6$  Hz, 1 H), 7.64 (d,  $J = 4.6$  Hz, 1 H), 7.85 (s, 1 H), 8.20 (s, 1 H).

**3-[1-(2-Methoxyethyl)-1H-pyrazol-4-yl]-8-morpholin-4-yl-2-(trifluoromethyl)imidazo[1,2-a]pyrazine (11)**. **11** was prepared according to a protocol analogous to that for compound **2** from **7e** and **12a**. Flash column chromatography (silica; 7 M solution of ammonia in MeOH in DCM, 0/100 to 2/98) yielded compound **11** as a pink solid (55%). UPLC/ESI-HRMS:  $m/z$  for  $C_{17}H_{20}F_3N_6O_2$  ( $M + H$ )<sup>+</sup> calcd 397.1600, found 397.1615 (3.8 ppm).  $t_R = 1.93$  min. <sup>1</sup>H NMR (500 MHz, DMSO- $d_6$ ):  $\delta$  (ppm) 3.26 (s, 3 H), 3.72–3.81 (m, 6 H), 4.18 (t,  $J = 4.3$  Hz, 4 H), 4.39 (t,  $J = 5.3$  Hz, 2 H), 7.51 (d,  $J = 4.6$  Hz, 1 H), 7.62 (d,  $J = 4.6$  Hz, 1 H), 7.78 (s, 1 H), 8.19 (s, 1 H).

**3-[1-(2-Methoxyethyl)-1H-pyrazol-4-yl]-8-morpholin-4-ylimidazo[1,2-a]pyrazine-2-carboxylic Acid Ethyl Ester (13)**. **13** was prepared according to a protocol analogous to that for compound **2** from **7f** and **12a**. Flash column chromatography (silica; MeOH in DCM, 0/100 to 10/90) and reversed-phase HPLC yielded **13** as a white solid (28%). MS:  $m/z$  401 [ $M + H$ ]<sup>+</sup>.  $t_R = 3.08$  min. <sup>1</sup>H NMR (500 MHz, DMSO- $d_6$ ):  $\delta$  (ppm) 1.23 (t,  $J = 7.1$  Hz, 3 H), 3.26 (s, 3 H), 3.76 (t,  $J = 4.5$  Hz, 6 H), 4.22 (br t,  $J = 4.0$ , 4 H), 4.25 (q,  $J = 6.9$  Hz, 2 H), 4.37 (t,  $J = 5.2$  Hz, 2 H), 7.43 (d,  $J = 4.9$  Hz, 1 H), 7.63 (d,  $J = 4.9$  Hz, 1 H), 7.84 (s, 1 H), 8.20 (s, 1 H).

**3-[1-(2-Methoxyethyl)-1H-pyrazol-4-yl]-8-morpholin-4-ylimidazo[1,2-a]pyrazine-2-carbonitrile (14)**. **Step 1: Synthesis of 3-[1-(2-methoxyethyl)-1H-pyrazol-4-yl]-8-morpholin-4-ylimidazo[1,2-a]pyrazine-2-carboxylic Acid amide**. **13** (0.3 g, 0.75 mmol) was dissolved in an ammonium hydroxide solution (5 mL). The mixture was stirred at 80 °C for 16 h, and then the solvent was evaporated in vacuo. The crude product was purified by flash column chromatography (silica; 7 M solution of ammonia in MeOH in DCM, 0/100 to 5/95). The desired fractions were collected, and the solvent was evaporated in vacuo to yield 3-[1-(2-methoxyethyl)-1H-pyrazol-4-yl]-8-morpholin-4-ylimidazo[1,2-a]pyrazine-2-carboxylic acid amide (0.31 g, 28%) as a white solid. MS:  $m/z$  372 [ $M + H$ ]<sup>+</sup>.  $t_R = 0.68$  min. <sup>1</sup>H NMR (500 MHz, CDCl<sub>3</sub>):  $\delta$  (ppm) 3.38 (s, 3 H), 3.83 (t,  $J = 5.2$  Hz, 2 H), 3.89 (dd,  $J = 5.2, 4.6$  Hz, 4 H), 4.28 (t,  $J = 4.6$  Hz, 4 H), 4.39 (t,  $J = 5.2$  Hz, 2 H), 5.52 (br s, 1 H), 7.14 (br s, 1 H), 7.40 (d,  $J = 4.6$  Hz, 1 H), 7.61 (d,  $J = 4.6$  Hz, 1 H), 7.88 (s, 1 H), 8.11 (s, 1 H). Mp: 195.3 °C.

**Step 2. Synthesis of 14**. A solution of 3-[1-(2-methoxyethyl)-1H-pyrazol-4-yl]-8-morpholin-4-ylimidazo[1,2-a]pyrazine-2-carboxylic

acid amide (0.13 g, 0.35 mmol) in phosphorus oxychloride (0.019 mL, 0.35 mmol) was stirred at 80 °C for 1 h. The mixture was allowed to cool to room temperature, then poured onto ice, basified by a saturated solution of sodium carbonate addition, and extracted with DCM. The organic layer was separated, dried (Na<sub>2</sub>SO<sub>4</sub>), and filtered, and the solvents were evaporated in vacuo. The crude product was purified by flash column chromatography (silica; MeOH in DCM, 0/100 to 2/98). The desired fractions were collected, and the solvent was evaporated in vacuo to yield **14** (0.048 g, 39%) as a white solid. UPLC/ESI-HRMS:  $m/z$  for  $C_{17}H_{20}N_7O_2$  ( $M + H$ )<sup>+</sup> calcd 354.1678, found 354.1681 (0.8 ppm).  $t_R = 1.50$  min. <sup>1</sup>H NMR (400 MHz, DMSO- $d_6$ ):  $\delta$  (ppm) 3.27 (s, 3 H), 3.68–3.85 (m, 6 H), 4.17 (m,  $J = 4.6$  Hz, 4 H), 4.42 (t,  $J = 5.3$  Hz, 2 H), 7.55 (d,  $J = 4.6$  Hz, 1 H), 7.83 (d,  $J = 4.6$  Hz, 1 H), 8.03 (s, 1 H), 8.44 (s, 1 H).

**2-Methoxy-3-[1-(2-methoxyethyl)-1H-pyrazol-4-yl]-8-morpholin-4-ylimidazo[1,2-a]pyrazine (17)**. **17** was prepared according to a protocol analogous to that for compound **2** from **7g** and **12a**. Flash column chromatography (silica; 7 M solution of ammonia in MeOH in DCM, 0/100 to 2/98) yielded compound **17** as a pink solid (38%). UPLC/ESI-HRMS:  $m/z$  for  $C_{17}H_{22}N_6O_3$  ( $M + H$ )<sup>+</sup> calcd 358.1754, found 359.1831 (−0.3 ppm).  $t_R = 1.57$  min. <sup>1</sup>H NMR (500 MHz, DMSO- $d_6$ ):  $\delta$  (ppm) 3.25 (s, 3 H), 3.72–3.81 (m, 6 H), 4.02 (s, 3 H), 4.08 (t,  $J = 4.6$  Hz, 4 H), 4.35 (t,  $J = 5.2$  Hz, 2 H), 7.51 (d,  $J = 4.3$  Hz, 1 H), 7.88 (d,  $J = 4.6$  Hz, 1 H), 7.91 (s, 1 H), 8.22 (s, 1 H).

**3-[1-(Cyclopropylmethyl)-1H-pyrazol-4-yl]-2-methyl-8-morpholin-4-ylimidazo[1,2-a]pyrazine (18)**. **18** was prepared according to a protocol analogous to that for compound **2** from **7b** and **12b**. Flash column chromatography (silica; 7 M solution of ammonia in MeOH in DCM, 1/99) and reversed-phase HPLC yielded compound **18** as a white solid (70%). UPLC/ESI-HRMS:  $m/z$  for  $C_{18}H_{23}N_6O$  ( $M + H$ )<sup>+</sup> calcd 339.1933, found 339.1934 (0.3 ppm).  $t_R = 1.71$  min. <sup>1</sup>H NMR (500 MHz, DMSO- $d_6$ ):  $\delta$  (ppm) 0.38–0.48 (m, 2 H), 0.51–0.63 (m, 2 H), 1.28–1.38 (m, 1 H), 2.40 (s, 3 H), 3.75 (t,  $J = 4.9$  Hz, 4 H), 4.07 (d,  $J = 7.2$  Hz, 2 H), 4.15 (t,  $J = 4.6$  Hz, 4 H), 7.38 (d,  $J = 4.6$  Hz, 1 H), 7.70 (d,  $J = 4.6$  Hz, 1 H), 7.80 (s, 1 H), 8.23 (s, 1 H).

**3-(1-Isopropyl-1H-pyrazol-4-yl)-2-methyl-8-morpholin-4-ylimidazo[1,2-a]pyrazine (19)**. **19** was prepared according to a protocol analogous to that for compound **2** from **7b** and **12c**. Reversed-phase HPLC yielded compound **19** as a yellow solid (61%). UPLC/ESI-HRMS:  $m/z$  for  $C_{17}H_{23}N_6O$  ( $M + H$ )<sup>+</sup> calcd 327.1933, found 327.1937 (1.2 ppm).  $t_R = 1.66$  min. <sup>1</sup>H NMR (300 MHz, CDCl<sub>3</sub>):  $\delta$  (ppm) 1.53 (d,  $J = 6.6$  Hz, 6 H), 2.36 (s, 3 H), 3.82 (t,  $J = 4.7$  Hz, 4 H), 4.17 (t,  $J = 4.7$  Hz, 4 H), 4.53 (spt,  $J = 6.6$  Hz, 1 H), 7.27 (d,  $J = 4.5$  Hz, 1 H), 7.38 (d,  $J = 4.5$  Hz, 1 H), 7.53 (s, 1 H), 7.61 (s, 1 H). Mp: 103.0–108.6 °C.

**3-(1-Isobutyl-1H-pyrazol-4-yl)-2-methyl-8-morpholin-4-ylimidazo[1,2-a]pyrazine (20)**. **20** was prepared according to a protocol analogous to that for compound **2** from **7b** and commercially available 1-isobutyl-4-(4,4,5,5-tetramethyl-1,3,2-dioxaborolan-2-yl)-1H-pyrazole (**12d**). Flash column chromatography (silica; AcOEt in heptane, 30/70 to 50/50) yielded compound **20** as a pale yellow solid (68%). UPLC/ESI-HRMS:  $m/z$  for  $C_{18}H_{25}N_6O$  ( $M + H$ )<sup>+</sup> calcd 341.2090, found 341.2121 (9.1 ppm).  $t_R = 1.94$  min. <sup>1</sup>H NMR (400 MHz, DMSO- $d_6$ ):  $\delta$  (ppm) 0.89 (d,  $J = 6.7$  Hz, 6 H), 2.19 (spt,  $J = 6.9$  Hz, 1 H), 2.38 (s, 3 H), 3.74 (t,  $J = 4.9$  Hz, 4 H), 4.02 (d,  $J = 7.2$  Hz, 2 H), 4.15 (t,  $J = 4.6$  Hz, 4 H), 7.37 (d,  $J = 4.6$  Hz, 1 H), 7.65 (d,  $J = 4.6$  Hz, 1 H), 7.80 (s, 1 H), 8.18 (s, 1 H). Mp: 83.65–87.69 °C.

**2-Methyl-8-morpholin-4-yl-3-[1-(2,2,2-trifluoroethyl)-1H-pyrazol-4-yl]imidazo[1,2-a]pyrazine (21)**. [1,1'-Bis-(diphenylphosphino)ferrocene]dichloropalladium(II) (0.002 g, 0.0013 mmol) was added to a mixture of **7b** (0.4 g, 1.35 mmol), **12e** (0.37 g, 1.35 mmol), and cesium carbonate (0.88 g, 2.7 mmol) in a mixture of 1,2-dimethoxyethane (6 mL) and water (2 mL) under nitrogen, and the mixture was stirred at 140 °C for 30 min under microwave irradiation. Then water (10 mL) was added and the mixture extracted with AcOEt. The organic layer was washed with brine, dried (Na<sub>2</sub>SO<sub>4</sub>), and concentrated in vacuo. The crude product was purified by reversed-phase HPLC to yield compound **21** as a white solid (0.252 g, 51%). UPLC/ESI-HRMS:  $m/z$  for  $C_{16}H_{18}F_3N_6O$  ( $M + H$ )<sup>+</sup> calcd 367.1493, found 367.1494 (0.3 ppm).  $t_R = 1.74$  min. <sup>1</sup>H

NMR (500 MHz, DMSO- $d_6$ ):  $\delta$  (ppm) 2.38 (s, 3 H), 3.75 (dd,  $J = 4.9$ , 4.3 Hz, 4 H), 4.15 (t,  $J = 4.6$  Hz, 4 H), 5.25 (q,  $J = 9.2$  Hz, 2 H), 7.39 (d,  $J = 4.6$  Hz, 1 H), 7.64 (d,  $J = 4.6$  Hz, 1 H), 7.98 (s, 1 H), 8.33 (s, 1 H). Mp: 137.9–138.9 °C.

**2-Methyl-8-morpholin-4-yl-3-[1-(2-fluoroethyl)-1H-pyrazol-4-yl]imidazo[1,2-*a*]pyrazine (22).** 22 was prepared according to a protocol analogous to that of compound 2 from 7b and 12f. Flash column chromatography (silica; AcOEt in heptane, 30/70 to 0/100) yielded compound 22 as a pale yellow solid (49%). UPLC/ESI-HRMS:  $m/z$  for  $C_{16}H_{20}FN_6O$  ( $M + H$ )<sup>+</sup> calcd 331.1682, found 331.1685 (0.9 ppm).  $t_R = 1.31$  min. <sup>1</sup>H NMR (400 MHz, CDCl<sub>3</sub>):  $\delta$  (ppm) 2.43 (s, 3 H), 3.95–3.83 (m, 4 H), 4.29–4.19 (m, 4 H), 4.60–4.43 (m, 2 H), 4.79 (t,  $J = 4.6$  Hz, 1 H), 4.91 (t,  $J = 4.6$  Hz, 1 H), 7.35 (d,  $J = 4.4$  Hz, 1 H), 7.43 (d,  $J = 4.6$  Hz, 1 H), 7.68 (s, 1 H), 7.72 (s, 1 H). Mp: 151.5 °C.

**3-[1-(2-Chlorobenzyl)-1H-pyrazol-4-yl]-2-methyl-8-morpholin-4-ylimidazo[1,2-*a*]pyrazine (23).** 23 was prepared according to a protocol analogous to that for compound 2 from 7b and 12g. Reversed-phase HPLC yielded compound 23 as a gray solid (34%). UPLC/ESI-HRMS:  $m/z$  for  $C_{21}H_{22}ClN_6O$  ( $M + H$ )<sup>+</sup> calcd 409.1543, found 409.1546 (0.7 ppm).  $t_R = 2.27$  min. <sup>1</sup>H NMR (300 MHz, CDCl<sub>3</sub>):  $\delta$  (ppm) 2.35 (s, 3 H), 3.81 (t,  $J = 4.5$  Hz, 4 H), 4.17 (t,  $J = 4.7$  Hz, 4 H), 5.46 (s, 2 H), 7.09–7.16 (m, 1 H), 7.21–7.26 (m, 2 H), 7.27 (d,  $J = 4.7$  Hz, 1 H), 7.35 (d,  $J = 4.5$  Hz, 1 H), 7.38 (dd,  $J = 4.3$ , 2.8 Hz, 1 H), 7.59 (s, 1 H), 7.66 (s, 1 H). Mp: 122.30–128.33 °C.

**2-Methyl-8-morpholin-4-yl-3-(1-pyridin-4-ylmethyl-1H-pyrazol-4-yl)imidazo[1,2-*a*]pyrazine (24).** 24 was prepared according to a protocol analogous to that for 2 from 7b and 12h. Flash column chromatography (silica; AcOEt in heptane, 30/70 to 100/0) yielded compound 24 as a beige solid (54%). UPLC/ESI-HRMS:  $m/z$  for  $C_{20}H_{22}N_7O$  ( $M + H$ )<sup>+</sup> calcd 376.1886, found 376.1886 (0.0 ppm).  $t_R = 1.33$  min. <sup>1</sup>H NMR (500 MHz, DMSO- $d_6$ ):  $\delta$  (ppm) 2.39 (s, 3 H), 3.65–3.78 (m, 4 H), 4.15 (d,  $J = 4.9$  Hz, 4 H), 5.51 (s, 2 H), 7.22 (d,  $J = 5.8$  Hz, 2 H), 7.33–7.42 (m, 1 H), 7.68–7.73 (m, 1 H), 7.90 (s, 1 H), 8.39 (s, 1 H), 8.56 (d,  $J = 5.8$  Hz, 2 H).

**3-[[4-(2-Methyl-8-morpholin-4-ylimidazo[1,2-*a*]pyrazin-3-yl)pyrazol-1-yl]methyl]isoquinoline (25).** 25 was prepared according to a protocol analogous to that for 2 from 7b and 12i. Flash column chromatography (silica; AcOEt in heptane, 60/40 to 100/0) yielded compound 25 as a solid (98%). UPLC/ESI-HRMS:  $m/z$  for  $C_{24}H_{24}N_7O$  ( $M + H$ )<sup>+</sup> calcd 426.2042, found 426.2047 (1.2 ppm).  $t_R = 1.98$  min. <sup>1</sup>H NMR (500 MHz, CDCl<sub>3</sub>):  $\delta$  (ppm) 2.43 (s, 3 H), 3.88 (t,  $J = 4.9$  Hz, 4 H), 4.24 (t,  $J = 4.6$  Hz, 4 H), 5.73 (s, 2 H), 7.30–7.36 (m, 2 H), 7.44 (d,  $J = 4.3$  Hz, 1 H), 7.58 (t,  $J = 7.5$  Hz, 1 H), 7.70–7.78 (m, 2 H), 7.80 (s, 1 H), 7.84 (d,  $J = 8.1$  Hz, 1 H), 8.09 (d,  $J = 8.4$  Hz, 1 H), 8.19 (d,  $J = 8.7$  Hz, 1 H).

**3-[1-(2-Methoxypropyl)-1H-pyrazol-4-yl]-2(S)-methyl-8-morpholin-4-ylimidazo[1,2-*a*]pyrazine (26).** 26 was prepared according to a protocol analogous to that for compound 2 from 7b and 12j. Flash column chromatography (silica; AcOEt in heptane, 70/30 to 100/0) and reversed-phase HPLC yielded compound 26 as a beige solid (56%). UPLC/ESI-HRMS:  $m/z$  for  $C_{18}H_{23}N_6O_2$  ( $M + H$ )<sup>+</sup> calcd 357.2039, found 357.2063 (6.7 ppm).  $t_R = 1.48$  min. <sup>1</sup>H NMR (500 MHz, DMSO- $d_6$ ):  $\delta$  (ppm) 1.10 (d,  $J = 6.4$  Hz, 3 H), 2.38 (s, 3 H), 3.21 (s, 3 H), 3.74 (br t,  $J = 4.6$  Hz, 4 H), 3.75–3.81 (m, 1 H), 4.15 (br t,  $J = 4.3$  Hz, 4 H), 4.22 (dd,  $J = 5.6$ , 2.5 Hz, 2 H), 7.38 (d,  $J = 4.6$  Hz, 1 H), 7.65 (d,  $J = 4.6$  Hz, 1 H), 7.81 (s, 1 H), 8.14 (s, 1 H).

**2-Methyl-8-morpholin-4-yl-3-(1H-pyrazol-4-yl)imidazo[1,2-*a*]pyrazine (28).** 28 was prepared according to a protocol analogous to that for compound 2 from 7b and commercially available 4-(4,4,5,5-tetramethyl-1,3,2-dioxaborolan-2-yl)pyrazole-1-carboxylic acid *tert*-butyl ester (27). Flash column chromatography (silica; AcOEt) yielded 28 as a solid (81%).

**3-[1-(2-Methoxy-2-methylpropyl)-1H-pyrazol-4-yl]-2-methyl-8-morpholin-4-ylimidazo[1,2-*a*]pyrazine (29).** *Step 1: Synthesis of 2-Methyl-1-[4-(2-methyl-8-morpholin-4-ylimidazo[1,2-*a*]pyrazin-3-yl)pyrazol-1-yl]propan-2-ol.* A mixture of 28 (0.10 g, 0.35 mmol), 1-chloro-2-methyl-2-propanol (0.05 g, 0.46 mmol), and cesium carbonate (0.17 g, 0.53 mmol) in DMF (3 mL) was stirred at 160 °C for 40 min under microwave irradiation. Then the mixture was concentrated in vacuo, and the residue was partitioned between

water and DCM. The organic layer was separated, dried (Na<sub>2</sub>SO<sub>4</sub>), and filtered, and the solvents were evaporated in vacuo. The crude product was purified by flash column chromatography (silica; 7 M solution of ammonia in MeOH in DCM, 1/99). The desired fractions were collected, and the solvent was evaporated in vacuo to yield 103 mg (82%) of 2-methyl-1-[4-(2-methyl-8-morpholin-4-ylimidazo[1,2-*a*]pyrazin-3-yl)pyrazol-1-yl]propan-2-ol as a colorless oil.

*Step 2. Synthesis of 29.* A 60% suspension of sodium hydride in mineral oils (163 mg, 4.09 mmol) was added to a stirred solution of 2-methyl-1-[4-(2-methyl-8-morpholin-4-ylimidazo[1,2-*a*]pyrazin-3-yl)pyrazol-1-yl]propan-2-ol (486 mg, 1.36 mmol) in THF (15 mL). The mixture was stirred at 0 °C for 5 min, and then dimethyl sulfate (0.324 mL, 4.86 mmol) was added. The mixture was stirred at 70 °C for 18 h. Then a saturated solution of NaHCO<sub>3</sub> was added. The organic layer was separated, dried (Na<sub>2</sub>SO<sub>4</sub>), and filtered, and the solvents were evaporated in vacuo. The crude product was purified twice by flash column chromatography (silica; 7 M solution of ammonia in MeOH in DCM, 1/99) and by reversed-phase HPLC. The desired fractions were collected, and the solvent was evaporated in vacuo to yield 29 (197 mg, 39%). UPLC/ESI-HRMS:  $m/z$  for  $C_{19}H_{27}N_6O_2$  ( $M + H$ )<sup>+</sup> calcd 371.2195, found 371.2208 (3.5 ppm).  $t_R = 1.67$  min. <sup>1</sup>H NMR (500 MHz, DMSO- $d_6$ ):  $\delta$  (ppm) 1.13 (s, 6 H), 2.38 (s, 3 H), 3.21 (s, 3 H), 3.75 (t,  $J = 4.9$  Hz, 4 H), 4.16 (t,  $J = 4.6$  Hz, 4 H), 4.23 (s, 2 H), 7.38 (d,  $J = 4.6$  Hz, 1 H), 7.64 (d,  $J = 4.3$  Hz, 1 H), 7.80 (s, 1 H), 8.05 (s, 1 H).

**3-(1-Ethyl-1H-pyrazol-4-yl)-2-methyl-8-morpholin-4-ylimidazo[1,2-*a*]pyrazine (30).** 30 was prepared according to a protocol analogous to that for 29 (step 1) from 28 and iodoethane. Flash column chromatography (silica; AcOEt in heptane, 50/50 to 100/0) yielded compound 30 (0.103 g, 62%) as a white solid. UPLC/ESI-HRMS:  $m/z$  for  $C_{16}H_{21}N_6O$  ( $M + H$ )<sup>+</sup> calcd 313.1777, found 313.1793 (5.1 ppm).  $t_R = 1.42$  min. <sup>1</sup>H NMR (500 MHz, DMSO- $d_6$ ):  $\delta$  (ppm) 1.45 (t,  $J = 7.2$  Hz, 3 H), 2.38 (s, 3 H), 3.74 (t,  $J = 4.6$  Hz, 4 H), 4.15 (t,  $J = 4.6$  Hz, 4 H), 4.24 (q,  $J = 7.2$  Hz, 2 H), 7.36 (d,  $J = 4.6$  Hz, 1 H), 7.69 (d,  $J = 4.3$  Hz, 1 H), 7.79 (s, 1 H), 8.19 (s, 1 H).

**3-Bromo-2-methyl-8-pyrrolidin-1-ylimidazo[1,2-*a*]pyrazine (31).** 31 was prepared according to a protocol analogous to that for 7a from 6b and pyrrolidine. Flash column chromatography (silica; AcOEt in DCM) yielded 31 as a white solid (85%).

**3-[1-(2-Methoxyethyl)-1H-pyrazol-4-yl]-2-methyl-8-pyrrolidin-1-ylimidazo[1,2-*a*]pyrazine (32).** 32 was prepared according to a protocol analogous to that for compound 2 from 31 and 12a. Flash column chromatography (silica; 7 M solution of ammonia in MeOH in DCM, 10/90) yielded compound 32 as a white solid (23%). UPLC/ESI-HRMS:  $m/z$  for  $C_{17}H_{23}N_6O$  ( $M + H$ )<sup>+</sup> calcd 327.1933, found 327.1938 (1.5 ppm).  $t_R = 1.57$  min. <sup>1</sup>H NMR (400 MHz, CDCl<sub>3</sub>):  $\delta$  (ppm) 1.97–2.05 (m, 4 H), 2.43 (s, 3 H), 3.38 (s, 3 H), 3.81 (t,  $J = 5.2$  Hz, 2 H), 4.05 (br s, 4 H), 4.39 (t,  $J = 5.2$  Hz, 2 H), 7.29 (s, 2 H), 7.68 (d,  $J = 5.3$  Hz, 2 H).

**2-Methyl-8-pyridin-4-ylimidazo[1,2-*a*]pyrazine (33a).** 33a was prepared according to a protocol analogous to that for compound 2 from 5b and 4-pyridylboronic acid. Flash column chromatography (silica; MeOH in DCM, 5/95) yielded 33a (53%) as a pale brown solid. MS:  $m/z$  211 [ $M + H$ ]<sup>+</sup>.  $t_R = 0.62$  min. <sup>1</sup>H NMR (400 MHz, CDCl<sub>3</sub>):  $\delta$  (ppm) 2.58 (d,  $J = 0.7$  Hz, 3 H), 7.55 (d,  $J = 0.7$  Hz, 1 H), 7.98 (d,  $J = 4.4$  Hz, 1 H), 8.05 (d,  $J = 4.4$  Hz, 1 H), 8.61 (dd,  $J = 4.4$ , 1.6 Hz, 2 H), 8.81 (dd,  $J = 4.4$ , 1.6 Hz, 2 H).

**2-Methyl-8-pyridin-3-ylimidazo[1,2-*a*]pyrazine (33b).** 33b was prepared according to a protocol analogous to that for compound 2 from 5b and 3-pyridylboronic acid. Flash column chromatography (silica; MeOH in DCM, 1/99) yielded 33b as a pale brown solid (63%). MS:  $m/z$  211 [ $M + H$ ]<sup>+</sup>.  $t_R = 0.75$  min. <sup>1</sup>H NMR (400 MHz, CDCl<sub>3</sub>):  $\delta$  (ppm) 2.57 (d,  $J = 0.5$  Hz, 3 H), 7.47 (ddd,  $J = 8.0$ , 4.8, 0.8 Hz, 1 H), 7.53 (s, 1 H), 7.96 (d,  $J = 4.4$  Hz, 1 H), 8.01 (d,  $J = 4.4$  Hz, 1 H), 8.72 (dd,  $J = 4.9$ , 1.6 Hz, 1 H), 9.04 (dt,  $J = 8.1$ , 2.0 Hz, 1 H), 9.84 (dd,  $J = 2.1$ , 0.7 Hz, 1 H).

**3-Bromo-2-methyl-8-pyridin-4-ylimidazo[1,2-*a*]pyrazine (34a).** 34a was prepared according to a protocol analogous to that for 6a from 33a. Precipitation from diethyl ether yielded 34a as a pale brown solid (86%). <sup>1</sup>H NMR (400 MHz, DMSO- $d_6$ ):  $\delta$  (ppm) 2.48 (s,

3 H) 8.17 (d,  $J = 4.4$  Hz, 1 H) 8.43 (d,  $J = 4.6$  Hz, 1 H) 8.60 (dd,  $J = 4.6, 1.6$  Hz, 2 H) 8.79 (dd,  $J = 4.4, 1.6$  Hz, 2 H).

**3-Bromo-2-methyl-8-pyridin-3-ylimidazo[1,2-*a*]pyrazine (34b).** 34b was prepared according to a protocol analogous to that for 6a from 33b. Precipitation from diethyl ether yielded 34b as a pale brown solid (89%). MS:  $m/z$  289  $[M + H]^+$ .  $t_R = 1.39$  min.  $^1H$  NMR (500 MHz,  $CDCl_3$ ):  $\delta$  (ppm) 2.57 (s, 3 H), 7.44–7.50 (m, 1 H), 8.01 (d,  $J = 4.6$  Hz, 1 H), 8.10 (d,  $J = 4.3$  Hz, 1 H), 8.73 (dd,  $J = 4.8, 1.6$  Hz, 1 H), 9.00 (dt,  $J = 8.1, 2.0$  Hz, 1 H), 9.84 (d,  $J = 1.4$  Hz, 1 H).

**3-[1-(2-Methoxyethyl)-1H-pyrazol-4-yl]-2-methyl-8-pyridin-4-ylimidazo[1,2-*a*]pyrazine (35).** 35 was prepared according to a protocol analogous to that for compound 2 from 34a and 12a. Flash column chromatography (silica; 7 M solution of ammonia in MeOH in DCM, 10/90) yielded compound 35 (48%) as a white solid. UPLC/ESI-HRMS:  $m/z$  for  $C_{18}H_{19}N_6O$   $(M + H)^+$  calcd 335.1620, found 335.1635 (4.5 ppm).  $t_R = 1.18$  min.  $^1H$  NMR (500 MHz,  $DMSO-d_6$ ):  $\delta$  (ppm) 2.56 (s, 3 H), 3.29 (s, 3 H), 3.80 (t,  $J = 5.3$  Hz, 2 H), 4.41 (t,  $J = 5.3$  Hz, 2 H), 7.96 (ddd,  $J = 8.0, 4.8, 0.8$  Hz, 1 H), 8.09 (d,  $J = 4.6$  Hz, 1 H), 8.32 (s, 1 H), 8.46 (d,  $J = 4.6$  Hz, 1 H), 8.70 (d,  $J = 6.1$  Hz, 2 H), 8.81 (d,  $J = 6.1$  Hz, 2 H).

**3-[1-(2-Methoxyethyl)-1H-pyrazol-4-yl]-2-methyl-8-pyridin-3-ylimidazo[1,2-*a*]pyrazine (36).** 36 was prepared according to a protocol analogous to that for compound 2 from 34b and 12a. Flash column chromatography (silica; 7 M solution of ammonia in MeOH in DCM, 10/90) yielded compound 36 as a solid (58%). UPLC/ESI-HRMS:  $m/z$  for  $C_{18}H_{19}N_6O$   $(M + H)^+$  calcd 335.1620, found 335.1621 (0.3 ppm).  $t_R = 1.14$  min.  $^1H$  NMR (400 MHz,  $DMSO-d_6$ ):  $\delta$  (ppm) 2.54 (s, 3 H), 3.28 (s, 3 H), 3.80 (t,  $J = 5.4$  Hz, 2 H), 4.40 (t,  $J = 5.4$  Hz, 2 H), 7.62 (ddd,  $J = 8.0, 4.8, 0.8$  Hz, 1 H), 7.96 (d,  $J = 0.7$  Hz, 1 H), 8.05 (d,  $J = 4.4$  Hz, 1 H), 8.31 (d,  $J = 0.7$  Hz, 1 H), 8.39 (d,  $J = 4.4$  Hz, 1 H), 8.72 (dd,  $J = 4.9, 1.6$  Hz, 1 H), 9.04 (dt,  $J = 8.0, 1.9$  Hz, 1 H), 9.85 (dd,  $J = 2.1, 0.7$  Hz, 1 H).

## ■ ASSOCIATED CONTENT

### Supporting Information

Crystal structure data, in vitro biology, pharmacology, and pharmacokinetics experimental details, and analytical methods. This material is available free of charge via the Internet at <http://pubs.acs.org>.

## ■ AUTHOR INFORMATION

### Corresponding Author

\*Phone: +34 925232331. Fax: +34 925245771. E-mail: [scondec@its.jnj.com](mailto:scondec@its.jnj.com).

### Notes

The authors declare no competing financial interest.

## ■ ACKNOWLEDGMENTS

We thank our co-workers Alberto Fontana, Alcira del Cerro, Herman Hendrickx, Koen Hens, and Ilse Lenaerts from the Discovery Sciences and Neuroscience Discovery teams and Allison Ritchie and Phil Leonard from Biofocus.

## ■ ABBREVIATIONS USED

ACN, acetonitrile; cAMP, cyclic adenosine monophosphate; AcOEt, ethyl acetate; APO, apomorphine; BTB, brain tissue binding; CNS, central nervous system; CYPs, cytochromes;  $D_1$ , dopamine 1;  $D_2$ , dopamine 2; DCM, dichloromethane; DAD, diode array; DIPEA, *N,N*-diisopropylethylamine; DME, 1,2-dimethoxyethane; DMF, *N,N*-dimethylformamide; DMSO, dimethyl sulfoxide; EPSs, extrapyramidal symptoms; MSNs, medium spiny neurons; EtOH, ethanol; GABA,  $\gamma$ -aminobutyric acid; Gln, glutamine; cGMP, cyclic guanosine monophosphate; h, hours; HPLC, high-performance liquid chromatography; UPLC, ultraperformance liquid chromatography;  $t_R$ , retention time (min); SQD, single-quadrupole detector; MSD, mass-

selective detector; TOF, time of flight; QTOF, quadrupole time of flight;  $[M + H]^+$ , protonated mass of the free base of the compound;  $[M - H]^-$ , deprotonated mass of the free base of the compound; HTS, high-throughput screening; MeOH, methanol; min, minutes; mp, melting point; mRNA, messenger ribonucleic acid; MS, mass spectrometry; MW, molecular weight; NBS, *N*-bromosuccinimide; NMR, nuclear magnetic resonance; PCP, phencyclidine; PDE, phosphodiesterase; Phe, phenylalanine; RLMS, rat liver microsomes; rPPB, rat plasma protein binding; rt, room temperature; SAR, structure–activity relationship; THF, tetrahydrofuran; TLC, thin-layer chromatography; TPSA, topological polar surface area; Thr, threonine; Trp, tryptophan

## ■ REFERENCES

- (1) Tandon, R.; Nasrallah, H. A.; Keshavan, M. S. Schizophrenia, “just the facts” 4. Clinical features and conceptualization. *Schizophr. Res.* **2009**, *110*, 1–23.
- (2) Seeman, P. Targeting the dopamine  $D_2$  receptor in schizophrenia. *Expert Opin. Ther. Targets* **2006**, *10*, 515–531.
- (3) Meltzer, H. Y. Treatment of schizophrenia and spectrum disorders: pharmacotherapy, psychosocial treatments, and neurotransmitter interactions. *Biol. Psychiatry* **1999**, *46*, 1321–1327.
- (4) Lieberman, J. A.; Stroup, T. S.; McEvoy, J. P.; Swartz, M. S.; Rosenheck, K. A.; Perkins, D. O.; Keefe, R. S.; Davis, S. M.; Davis, C. E.; Lebowitz, B. D.; Severe, J.; Hsiao, J. K.; Adler, L.; Bari, M.; Belz, L.; Bland, R.; Blocher, T.; Bolyard, B.; Buffenstein, A.; Burruss, J.; Byerly, M.; Canive, J.; Caroff, S.; Casat, C.; Chavez-Rice, E.; Csernansky, J.; Delgado, P.; Douyon, R.; D'Souza, C.; Glick, I.; Goff, D.; Gratz, S.; Grossberg, G. T.; Hale, M.; Hamner, M.; Jaffe, R.; Jeste, D.; Kablinger, A.; Khan, A.; Lambert, S.; Levy, M. T.; Lieberman, J. A.; Maguire, G.; Manschreck, T.; McEvoy, J.; McGee, M.; Meltzer, H.; Miller, A.; Miller, D. D.; Nastrallah, H.; Nemeroff, C.; Olson, S.; Oxenkrug, G. F.; Patel, J.; Reimherr, F.; Riggio, S.; Risch, S.; Saltz, B.; Simpatico, T.; Simpson, G.; Smith, M.; Sommi, R.; Steinbook, R. M.; Stevens, M.; Tapp, A.; Torres, R.; Weiden, P.; Wolberg, J. Effectiveness of antipsychotic drugs in patients with chronic schizophrenia. *N. Engl. J. Med.* **2005**, *353*, 1209–1223.
- (5) Macdonald, G. J.; Bartolome, J. M. A decade of progress in the discovery and development of ‘atypical’ antipsychotics. *Prog. Med. Chem.* **2010**, *49*, 37–80.
- (6) (a) Kehler, J.; Ritzén, A.; Greve, D. R. The potential therapeutic use of phosphodiesterase 10 inhibitors. *Expert Opin. Ther. Patents* **2007**, *17*, 147–158. (b) Bender, A. T.; Beavo, J. A. Cyclic nucleotide phosphodiesterases: molecular regulation to clinical use. *Pharmacol. Rev.* **2006**, *58*, 488–520. (c) Grauer, S. M.; Pulito, V. L.; Navarra, R. L.; Kelly, M. P.; Kelley, C.; Graf, R.; Langen, B.; Logue, S.; Brennan, J.; Jiang, L.; Charych, E.; Egerland, U.; Liu, F.; Marquis, K. L.; Malamas, M.; Hage, T.; Comery, T. A.; Brandon, N. J. Phosphodiesterase 10A inhibitor activity in preclinical models of the positive, cognitive, and negative symptoms of schizophrenia. *J. Pharmacol. Exp. Ther.* **2009**, *331* (2), 574–590. (d) Blokland, A.; Menniti, F. S.; Prickaerts, J. PDE inhibition and cognition enhancement. *Expert Opin. Ther. Patents* **2012**, *22* (4), 349–354.
- (7) (a) Soderling, S. H.; Bayuga, S. J.; Beavo, J. A. Isolation and characterization of a dual-substrate phosphodiesterase gene family: PDE10A. *Proc. Natl. Acad. Sci. U.S.A.* **1999**, *96*, 7071–7076. (b) Fujishige, K.; Kotera, J.; Michibata, H.; Yuasa, K.; Takebayashi, S.-I.; Okumura, K.; Omori, K. Cloning and characterization of a novel human phosphodiesterase that hydrolyzes both cAMP and cGMP (PDE10A). *J. Biol. Chem.* **1999**, *274*, 18438–18445. (c) Loughney, K.; Snyder, P. B.; Uher, L.; Rosman, G. J.; Ferguson, K.; Florio, V. A. Isolation and characterization of PDE10A, a novel human 3',5'-cyclic nucleotide phosphodiesterase. *Gene* **1999**, *234*, 109–117.
- (8) High mRNA expression in testes in rat: Fujishige, K.; Kotera, J.; Omori, K. Striatum- and testis-specific phosphodiesterase PDE10A: isolation and characterization of a rat PDE10A. *Eur. J. Biochem.* **1999**,

266, 1118–1127. However, no protein staining in rat nor in human (some in mice and monkey): Coskran, T. M.; Morton, D.; Menniti, F. S.; Adamowicz, W. O.; Kleiman, R. J.; Ryan, A. M.; Strick, C. A.; Schmidt, C. J.; Stephenson, D. T. Immunohistochemical localization of phosphodiesterase 10A in multiple mammalian species. *J. Histochem. Cytochem.* **2006**, *54*, 1205–1213.

(9) Seeger, T. F.; Bartlett, B.; Coskran, T. M.; Culp, J. S.; James, L. C.; Krull, D. L.; Lanfear, J.; Ryan, A. M.; Schmidt, C. J.; Strick, C. A.; Varghese, A. H.; Williams, R. D.; Wylie, P. G.; Menniti, F. S. Immunohistochemical localization of PDE10A in the rat brain. *Brain Res.* **2003**, *985*, 113–126.

(10) Menniti, F. S.; Chappie, T. A.; Humphrey, J. M.; Schmidt, C. J. Phosphodiesterase 10A inhibitors: a novel approach to the treatment of the symptoms of schizophrenia. *Curr. Opin. Invest. Drugs* **2007**, *8* (1), 54–59.

(11) Siuciak, J. A.; Chapin, D. S.; Harms, J. F.; Lebel, L. A.; McCarthy, S. A.; Chambers, L.; Shrikhande, A.; Wong, S.; Menniti, F. S.; Schmidt, C. J. Inhibition of the striatum-enriched phosphodiesterase PDE10A: a novel approach to the treatment of psychosis. *Neuropharmacology* **2006**, *51*, 386–396.

(12) Chappie, T. A.; Helal, C. J.; Hou, X. J. The current landscape of phosphodiesterase 10A (PDE10A) inhibition. *J. Med. Chem.* **2012**, *55* (17), 7299–7331.

(13) Schmidt, C. J.; Chapin, D. S.; Cianfrogna, J.; Corman, M. L.; Hajos, M.; Harms, J. F.; Hoffman, W. E.; Lebel, L. A.; McCarthy, S. A.; Nelson, F. R.; Proulx-LaFrance, C.; Majchrzak, M. J.; Ramirez, A. D.; Schmidt, K.; Seymour, P. A.; Siuciak, J. A.; Tingley, F. D.; Williams, R. D.; Verhoest, P. R.; Menniti, F. S. Preclinical characterization of selective phosphodiesterase 10A inhibitors: a new therapeutic approach to the treatment of schizophrenia. *J. Pharmacol. Exp. Ther.* **2008**, *325*, 681–690.

(14) (a) Verhoest, P. R.; Chapin, D. S.; Corman, M.; Fonseca, K.; Harms, J. F.; Hou, X.; Marr, E. S.; Menniti, F. S.; Nelson, F.; O'Connor, R.; Pandit, J.; Proulx-LaFrance, C.; Schmidt, A. W.; Schmidt, C. J.; Siuciak, J. A.; Liras, S. Discovery of a novel class of phosphodiesterase 10A inhibitors and identification of clinical candidate 2-[4-(1-methyl-4-pyridin-4-yl-1H-pyrazol-3-yl)-phenoxy-methyl]-quinoline (PF-2545920)(I) for the treatment of schizophrenia. *J. Med. Chem.* **2009**, *52*, 5188–5196. (b) Malamas, M. S.; Ni, Y.-K.; Erdei, J.; Stange, H.; Schindler, R.; Lankau, H.-J.; Grunwald, C.; Fan, K. Y.; Parris, K.; Langen, B.; Egerland, U.; Hage, T.; Marquis, K. L.; Grauer, S.; Brennan, J.; Navarra, R.; Graf, R.; Harrison, B. L.; Robichaud, A.; Kronbach, T.; Pangalos, M. N.; Hoefgen, N.; Brandon, N. J. Highly potent, selective, and orally active phosphodiesterase 10A inhibitors. *J. Med. Chem.* **2011**, *54*, 7621–7638. (c) Yang, S.-W.; Smotryski, J.; McElroy, W. T.; Tan, Z.; Ho, G.; Tulshian, D.; Greenlee, W. J.; Guzzi, M.; Zhang, X.; Mullins, D.; Xiao, L.; Hruza, A.; Chan, T.-M.; Rindgen, D.; Bleickardt, C.; Hodgson, R. Discovery of orally active pyrazoloquinolines as potent PDE10 inhibitors for the management of schizophrenia. *Bioorg. Med. Chem. Lett.* **2012**, *22*, 235–239. (d) Ho, G. D.; Yang, S.-W.; Smotryski, J.; Bercovici, A.; Nechuta, T.; Smith, E. M.; McElroy, W.; Tan, Z.; Tulshian, D.; McKittrick, B.; Greenlee, W. J.; Hruza, A.; Xiao, L.; Rindgen, D.; Mullins, D.; Guzzi, M.; Zhang, X.; Bleickardt, C.; Hodgson, R. The discovery of potent, selective, and orally active pyrazoloquinolines as PDE10A inhibitors for the treatment of schizophrenia. *Bioorg. Med. Chem. Lett.* **2012**, *22*, 1019–1022. (e) McElroy, W. T.; Tan, Z.; Basu, K.; Yang, S.-W.; Smotryski, J.; Ho, G. D.; Tulshian, D.; Greenlee, W. J.; Mullins, D.; Guzzi, M.; Zhang, X.; Bleickardt, C.; Hodgson, R. Pyrazoloquinolines as PDE10A inhibitors: discovery of a tool compound. *Bioorg. Med. Chem. Lett.* **2012**, *22*, 1335–1339. (f) Hu, E.; Kunz, R. K.; Rumpf, S.; Chen, N.; Bürl, R.; Li, C.; Andrews, K. L.; Zhang, J.; Chmait, S.; Kogan, J.; Lindstrom, M.; Hitchcock, S. A.; Treanor, J. Discovery of potent, selective, and metabolically stable 4-(pyridin-3-yl)cinnolines as novel phosphodiesterase 10A (PDE10A) inhibitors. *Bioorg. Med. Chem. Lett.* **2012**, *22*, 2262–2265. (g) Ho, G. D.; Seganish, W. M.; Bercovici, A.; Tulshian, D.; Greenlee, W. J.; Van Rijn, R.; Hruza, A.; Xiao, L.; Rindgen, D.; Mullins, D.; Guzzi, M.; Zhang, X.; Bleickardt, C.; Hodgson, R. The SAR development of dihydroimidazoisoquinoline

derivatives as phosphodiesterase 10A inhibitors for the treatment of schizophrenia. *Bioorg. Med. Chem. Lett.* **2012**, *22*, 2585–2589. (h) Hoefgen, N.; Stange, H.; Schindler, R.; Lankau, H.-J.; Grunwald, C.; Langen, B.; Egerland, U.; Tremmel, P.; Pangalos, M. N.; Marquis, K. L.; Hage, T.; Harrison, B. L.; Malamas, M. S.; Brandon, N. J.; Kronbach, T. Discovery of imidazo[1,5-*a*]pyrido[3,2-*e*]pyrazines as a new class of phosphodiesterase 10A inhibitors. *J. Med. Chem.* **2010**, *53* (11), 4399–4411.

(15) Verhoest, R. P. *Abstracts of Papers*, 236th ACS National Meeting, Philadelphia, PA, Aug 17–21, 2008; American Chemical Society: Washington, DC, 2008; Abstract MEDI 219.

(16) DeMartinis, N.; Banerjee, A.; Kumar, V.; Boyer, S.; Schmidt, C.; Arroyo, S. Poster 212. Results of a Phase IIa proof-of-concept trial with a PDE10A inhibitor in the treatment of acute exacerbation of schizophrenia. *Schizophr. Res.* **2012**, *136*, 262.

(17) According to ClinicalTrials.gov, Pfizer is currently recruiting for a study to examine the safety, tolerability, and pharmacokinetics of PF02545920 in psychiatrically stable subjects with schizophrenia and is planning to recruit for three studies: a study to evaluate the PDE10 enzyme occupancy following a single dose of PF02545920 in healthy male volunteers (PET), an outpatient study of the efficacy, safety, and tolerability of PF02545920 in the adjunctive treatment of suboptimally controlled symptoms of schizophrenia, and a study evaluating the safety, tolerability, and brain function of two doses of PF02545920 in subjects with early Huntington's disease.

(18) According to the Thomson Reuters Integrity database, four compounds are currently undergoing clinical trials: Tak063, RG-7203, and AMG-579 in phase I for the treatment of schizophrenia and OMS-824 for the treatment of HD. Recently, Omeros has disclosed positive data on the phase I trial and plans to advance OMS824 into phase 2 trials, focusing initially on HD and following a phase 2a trial in patients with schizophrenia shortly thereafter.

(19) Leuti, A.; Laurenti, D.; Giampa, C.; Montagna, E.; Dato, C.; Anzilotti, S.; Melone, M.; Bernardi, G.; Fusco, F. R. Phosphodiesterase 10A (PDE10A) localization in the R6/2 mouse model of Huntington's disease. *Neurobiol. Dis.* **2013**, *52*, 104–116. (b) C. Giampa, C.; Laurenti, D.; Anzilotti, S.; Bernardi, G.; Menniti, F. S.; Fusco, F. R. Inhibition of the striatal specific phosphodiesterase PDE10A ameliorates striatal and cortical pathology in R6/2 mouse model of Huntington's disease. *PLoS One* **2010**, *5*, e13417. (c) Kleiman, R. J.; Kimmel, L. H.; Bove, S. E.; Lanz, T. A.; Harms, J. F.; Romegialli, A.; Miller, K. S.; Willis, A.; des Etages, S.; Max Kuhn, M.; Christopher, J.; Schmidt, C. J. Chronic suppression of phosphodiesterase 10A alters striatal expression of genes responsible for neurotransmitter synthesis, neurotransmission, and signaling pathways implicated in Huntington's disease. *J. Pharmacol. Exp. Ther.* **2011**, *336* (Jan), 64–76.

(20) Guibinga, G.-H.; Fiona, M.; Barron, N. HPRT-deficiency dysregulates cAMP-PKA signaling and phosphodiesterase 10A expression: mechanistic insight and potential target for Lesch-Nyhan disease? *PLoS One* **2013**, *8* (5), e63333.

(21) Belanger, D. B.; Curran, P. J.; Hruza, A.; Voigt, J.; Meng, Z.; Mandal, A. K.; Siddiqui, M. A.; Basso, A. D.; Gray, K. Discovery of imidazo[1,2-*a*]pyrazine-based aurora kinase inhibitors. *Bioorg. Med. Chem. Lett.* **2010**, *20* (17), 5170–5174.

(22) (a) Card, G. L.; England, B. P.; Suzuki, Y.; Fong, D.; Powell, B.; Lee, B.; Luu, C.; Tabrizizad, M.; Gillette, S.; Ibrahim, P. M.; Artis, D. R.; Bollag, G.; Milburn, M. V.; Kim, S. H.; Schlessinger, J.; Zhang, K. J. Y. Structural basis for the activity of drugs that inhibit phosphodiesterases. *Structure* **2004**, *12*, 2233–2247. (b) Manallack, D. T.; Hughes, R. A.; Thompson, P. E. The next generation of phosphodiesterase inhibitors: structural clues to ligand and substrate selectivity of phosphodiesterases. *J. Med. Chem.* **2005**, *48* (10), 3449–3462. (c) Zhang, K.Y. J.; Card, G. L.; Suzuki, Y.; Artis, D. R.; Fong, D.; Gillette, S.; Hsieh, D.; Neiman, J.; West, B. L.; Zhang, C.; Milburn, M. V.; Kim, S.-H.; Schlessinger, J.; Bollag, G. A glutamine switch mechanism for nucleotide selectivity by phosphodiesterases. *Mol. Cell* **2004**, *15* (2), 279–286. (d) Lau, J.; Xiao-Bo, Li; Yuen-Kit, C. A substrate selectivity and inhibitor design lesson from the PDE10-

cAMP crystal structure: a computational study. *J. Phys. Chem. B* **2010**, *114* (15), 5154–5160.

(23) Chemical Computing Group Inc. (Montreal, Canada). Molecular Operating Environment (MOE) v2012.10, 2012. Available at <http://www.chemcomp.com>.

(24) The 2D representation has been proposed by Chappie et al.: Chappie, T. A.; Helal, C. J.; Hou, X. J. The current landscape of phosphodiesterase 10A (PDE10A) inhibition. *J. Med. Chem.* **2012**, *55* (17), 7299–7331.

(25) Langlois, X.; Megens, A.; Lavreysen, H.; Atack, J.; Cik, M.; Te Riele, P.; Peeters, L.; Wouters, R.; Vermeire, J.; Hendrickx, H.; Macdonald, G.; De Bruyn, M. Pharmacology of JNJ-37822681, a specific and fast-dissociating D<sub>2</sub> antagonist for the treatment of schizophrenia. *J. Pharmacol. Exp. Ther.* **2012**, *342* (1), 91–105.

(26) Bartolome-Nebreda, J. M.; Conde-Ceide, S.; MacDonald, G. J.; Pastor-Fernandez, J.; Van Gool, L. M.; Martin-Martin, M. L.; Vanhoof, G. C. P. PCT Int. Appl. WO2011 110545A12011091, 2011.

(27) Chappie, T. A.; Humphrey, J. M.; Allen, M. P.; Estep, K. G.; Fox, C. B.; Lebel, L. A.; Liras, S.; Marr, E. S.; Menniti, F. S.; Pandit, J.; Schmidt, C. J.; Tu, M.; Williams, R. D.; Yang, F. V. Discovery of a series of 6,7-dimethoxy-4-pyrrolidylquinazoline PDE10A inhibitors. *J. Med. Chem.* **2007**, *50* (2), 182–185.

(28) PDB code 3HR1.

(29) Gleason, S. D.; Shannon, H. E. Blockade of phencyclidine-induced hyperlocomotion by olanzapine, clozapine and serotonin receptor subtype selective antagonists in mice. *Psychopharmacology* **1997**, *129*, 79–84.

(30) Celen, S.; Koole, M.; De Angelis, M.; Sannen, I.; Chitneni, S.; Alcazar, J.; Dedeurwaerdere, S.; Moechars, D.; Schmidt, M.; Verbruggen, A.; Langlois, X.; Laere, K.; Andres, J. I.; Bormans, G. Preclinical evaluation of 18F-JNJ41510417 as a radioligand for PET Imaging of phosphodiesterase-10A in the brain. *J. Nucl. Med.* **2010**, *51*, 1584–1591.

(31) Gaudry, M.; Marquet, M. 1-Bromo-3-methyl-2-butanone. *Org. Synth.* **1976**, *55*, 24–26.